ANALYSIS OF CHEMICALLY-ACTIVATED PATHWAYS FOR MOLECULAR WEIGHT GROWTH

Anthony M. Dean
Exxon Research and Engineering Company
P. O. Box 998, Annandale, NJ 08801
and
Joseph W. Bozzelli
Department of Chemical Engineering and Chemistry
NJIT, Newark, NJ 07039

Keywords: Chemical activation, rapid molecular weight growth, kinetic mechanisms

The unusually rapid rate of molecular weight growth in high temperature pyrolysis and oxidation of hydrocarbons has presented a substantial challenge to kineticists. Although there has been progress recently in characterization of the rapid rate of growth, attempts to accurately model the process have been only partially successful. For example, the extensive study of Frenklach et al[1] required rate constants for radical addition reactions which are several orders of magnitude larger than usually observed for these types of reactions.

There appear to be three possible pathways to rapid molecular growth:

(1) Diels-Alder cycloadditions reactions
(2) Ion-molecule reactions with their very large rate constants
(3) Radical addition to unsaturates

A major difficulty with (1) is that the equilibrium constants for this type of reaction suggest that the cyclic product would tend to dissociate to the linear fragments at high temperatures where the fast growth is observed. Ionic mechanisms are suspect since rapid growth is observed under pyrolytic conditions where the ion concentration would be expected to be extremely low. By default, then, our attention (like Frenklach et al) have focussed upon radical addition reactions. Previously, we demonstrated[2] that new reaction channels could open up at higher temperatures in chemically-activated reactions like those involving radical addition to unsaturates.

The methane pyrolysis data of Back and Back[3] provided an opportunity to see if properly accounting for chemical activation might explain the observed sharp increase in rate of reaction at very low extents of conversion at temperatures near 1000K. It was possible to explain the observed acceleration[4] and to demonstrate that a critical feature of the mechanism was the very rapid production of cyclopentadiene via chemically-activated pathways. These chemically-activated adducts have enough internal energy to react unimolecularly before collisional stabilization can occur; this significantly increases the overall rate of production of heavier species because no time is required for collisional deactivation and subsequent activation to get to the same products.

This analysis also led to some useful generalizations about features of potential energy surfaces which can lead to rapid growth. Specifically, it was found that allyl addition to acetylene was critical, while the analogous addition to ethylene was not

important, even though ethylene was present in much larger concentrations. Fig. 1 compares the potential surfaces for these two reactions. Note the differences in the energetics. First the well for acetylene addition is deeper by 8 kcal/mole. Furthermore, the difference in energy between the linear and cyclic intermediates is greater in the acetylene case by about 9 kcal/mole. Much of this difference can be attributed the the relatively high energy vinyllic radical (C=CCC=C•). Even with respect to final products, the acetylene is overall exothermic while ethylene is endothermic. Each of these differences contribute to the enhancement for the acetylene reaction. The shallower well for ethylene addition will contribute to more stabilization since the barrier to cyclization is comparable to the entrance channel, while for acetylene the cyclization barrier is 11 kcal/mole lower. Similarly, the difference in energy between linear and cyclic intermediates means that the equilibrium constant for the cyclization involving C=CCC=C• is more favorable, i. e., by a factor of 60 at 1038K (the temperature of the Back and Back experiments), than for the cyclization of C=CCCC•. Thus we expect cyclization, whether it occurs via stabilized or energized adducts, to be much more favored for the case of C=CCC=C•; under the present conditions, this difference is enough to make contributions from allyl addition to ethylene unimportant. In general, the shallower wells in the ethylene system, coupled with the greater entropy of the reactants relative to the intermediates, favor redissociation of the adducts back to reactants, thus making this an inefficient channel for molecular weight growth.

These observations can be generalized to other addition reactions. The following factors should increase the probability that direct production of cyclic species can occur via an energized-complex mechanism:

(1) A deep well for the linear adduct—this will tend to make the barrier to cyclization lower than the entrance barrier, thus increasing its unimolecular rate.
(2) An increase in the exothermicity of the cyclization reaction—this is needed to offset the entropy loss upon cyclization.
(3) A final cyclic product with high stability—this will result in low energy exit channels relative to the entrance and will lead to faster unimolecular rates.

One such system where these factors are especially significant is the formation of benzene via the sequence:

$$1\text{-}C_4H_5 + C_2H_2 = 1\text{-}C_6H_7 = \text{cyclohexadienyl} = \text{benzene} + H. \qquad \textbf{(A)}$$

The potential energy diagram is shown in Fig. 2. Here the linear adduct is seen to gave a much deeper well than that resulting from the allylic addition shown in Fig. 1. Here the adding radical is vinyllic, as contrasted to the resonantly stabilized allyl; thus there is no loss of resonance upon addition as is the case with allyllic species. The cyclization is also much more favored in the benzene system since the combination of an unstable vinyllic linear radical and a very stable cyclic radical results in an exothermicity of 43 kcal/mole for the cyclization. Furthermore, note that the final exit channel for benzene production, due to its unusual stability as an aromatic molecule, is much lower than the entrance channel. As a result, this path to benzene can be very important. In fact, at 1 atm and 1200K, the rate of production of benzene via the direct reaction of the energized complex accounts for over 90% of the total reaction of the initially formed linear adduct. Here the overall exothermicity is sufficient to

compensate for the loss in entropy upon cyclization. Such compensation is particularly important at high temperatures where the $T_{\Delta}S$ term plays a larger role.

Another interesting issue in molecular weight growth is the possibility of isomerization of methyl-cyclic C_5 compounds to cyclic C_6 compounds. Such isomerizations were considered in chlorobenzene pyrolysis to explain observed production of minor amounts of cyclopentadiene[5]. Given the prediction of cyclopentadiene production in methane pyrolysis, Fig. 3 suggests a possible route to benzene from cyclopentadiene. The recombination of the cyclopentadienyl radical with methyl is quite likely in these systems since both species are likely to build up to quite high concentrations, relative to other radicals, since the are no facile dissociation chaannels available. Note the production of methyl-cyclopentadienyl is only 8 kcal/mole endothermic. Once formed it can undergo beta-scission to form fulvalene. H-atom addition to the fulvalene (to the opposite end of the double bond) leads to the cyclopentadienylmethyl radical, which would be expected to quickly convert, over a series of low barriers, to benzene. This analysis would suggest that one really needs to consider formation of both 5 and 6 membered rings as the starting points for aromatics formation.

In an effort to better understand the detailed kinetics of molecular weight growth, we have used a molecular-beam sampling mass spectrometer (MBMS) to directly observe reactants, products, and reactive intermediates in hydrocarbon pyrolysis and oxidation[6]. A key component of this approach is use of photoionization at 10.5 ev., obtained by tripling the tripled (355 nm) out of a YAG laser. It is then possible to minimize fragmentation, substantially improving one's ability to observe free radicals that would otherwise be obscured by parent fragments. A schematic of the experimental set-up along with typical data from 1-butene pyrolysis is shown in Fig. 4. This system has been used to observe the production of both C_5 and C_6 species during pyrolysis and oxidation of C_4 molecules. In a typical experiment, the temperature is slowly increased at constant residence time and the molecular weight growth is monitored as one goes to higher conversions. A particularly interesting observation was that the allyl radical concentration was observed to decline at temperatures where C_5 and C_6 molecules were initially observed to be produced. We are now comparing these results with our detailed models of molecular weight growth.

An analysis of benzene production in low pressure flames[7] led to the identification of several radical addition reactions that might account for the observed production. One such path was that considered above in **(A)**. This path was chosen by comparison of the measured concentrations C_4H_5 and C_2H_2 to the rate of benzene production. However, since C_4H_5 was measured with a mass spectrometer, it was not possible to distinguish 1-C_4H_5 from 2-C_4H_5. If these two isomers were equilibrated and if the secondary radical were much more stable, one would expect the majority of the measured C_4H_5 to be the secondary radical, which is not expected to rapidly form benzene, and this particular route would be unimportant. [However, it is important to note that the secondary radical can add to acetylene to form a fulvalene radical, and thus it might be converted to benzene in a second step, as discussed above.] Thus a critical issue, as yet not completely resolved, is the relative stability of these two isomers. At first glance, it might appear that the secondary radical would be much more stable, since the unpaired electron could be stabilized by the adjacent double bond. Indeed, The Sandia Thermodynamic database[8] indicates a normal resonance

stabilization (12 kcal/mole) in the secondary radical. However, the rotation required here would disrupt the conjugation in the system as well as result in the relatively high energy allenic structure (1,2 butadiene is 12.5 kcal/mole less stable that 1,3 butadiene[9]). Thus, it might appear that the normal resonance stabilization could be offset, and the energies of two isomers could be quite close. We feel this is an area which warrants further investigation. For the flame work considered here, benzene production occurs near 1500K. This implies that a difference in stability of 3 kcal/mole in the two isomeric forms would result in 42% of the C_4H_5 as the primary isomer, meaning that this could be a major route to benzene. However, a difference of 12 kcal/mole, i. e., a typical resonance stabilization energy, would mean that only 4% of the primary isomer would be present at equilibrium; thus ruling out this direct path to benzene in this flame.

(1) Frenklach, M.; Clary, D. W.; Gardiner, W. C., Jr.; Stein, S. In *Twenty-first Symposium (International) on Combustion*; The Combustion Institute: 1986; pp 1067-1076.
(2) Dean, A. M. *J. Phys. Chem.* **1985**, *89*, 4600.
(3) Back, M. H.; Back, R. A. In *Pyrolysis: Theory and Industrial Practice*; L. F. Albright, B. L. Crynes and W. H. Corcoran, Ed.; Academic Press: New York, 1983; pp 1-24.
(4) Dean, A. M. *J. Phys. Chem.* **1990**, *94*, 1432-39.
(5) Ritter, E.; Dean, A. M.; Bozzelli, J. W. *J. Phys. Chem.* **1990**, *94*, 2493-2504.
(6) Woodin, R. L.; Dean, A. M.; Kearsley, T., Paul, A.; Zhong, X.; Mancuso, J. In *Second International Conference on Chemical Kinetics*; Gaithersburg, MD, 1989.
(7) Westmoreland, P. R.; Dean, A. M.; Howard, J. B.; Longwell, J. P. *J. Phys. Chem.* **1989**, *93*, 8171-80.
(8) Kee, R. J.; Rupley, F. M.; Miller, J. A. "The Chemkin Thermodynamic Data Base," Sandia National Lab, 1990.
(9) Pedley, J. B.; Naylor, R. O.; Kirby, S. P. *Thermodynamic Data of Organic Compounds*; Chapman and Hall: New York, 1987.

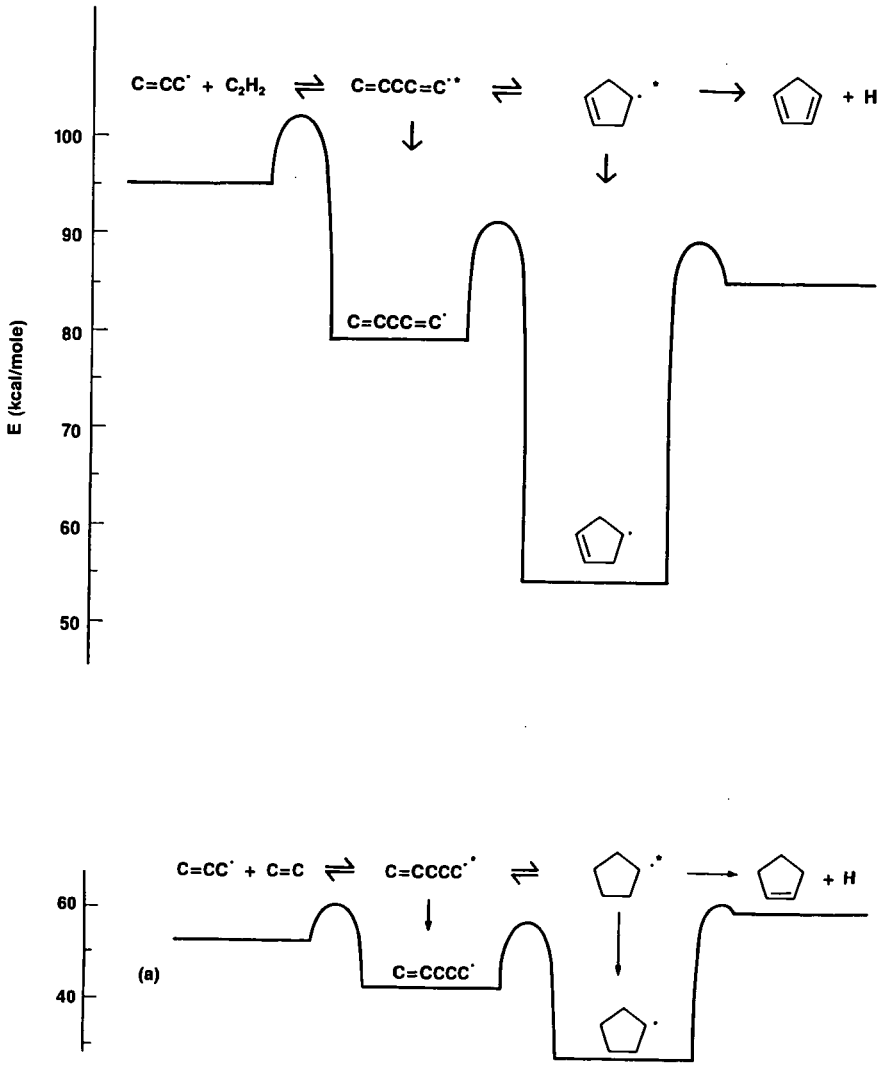
C=CC· + C2H2
C=CCC=C·
+ H
C=CCC=C·
E (kcal/mole)
100
90
80
70
60
50
C=CC· + C=C
C=CCCC·
+ H
C=CCCC·
(a)
60
40

Figure 1

Figure 2

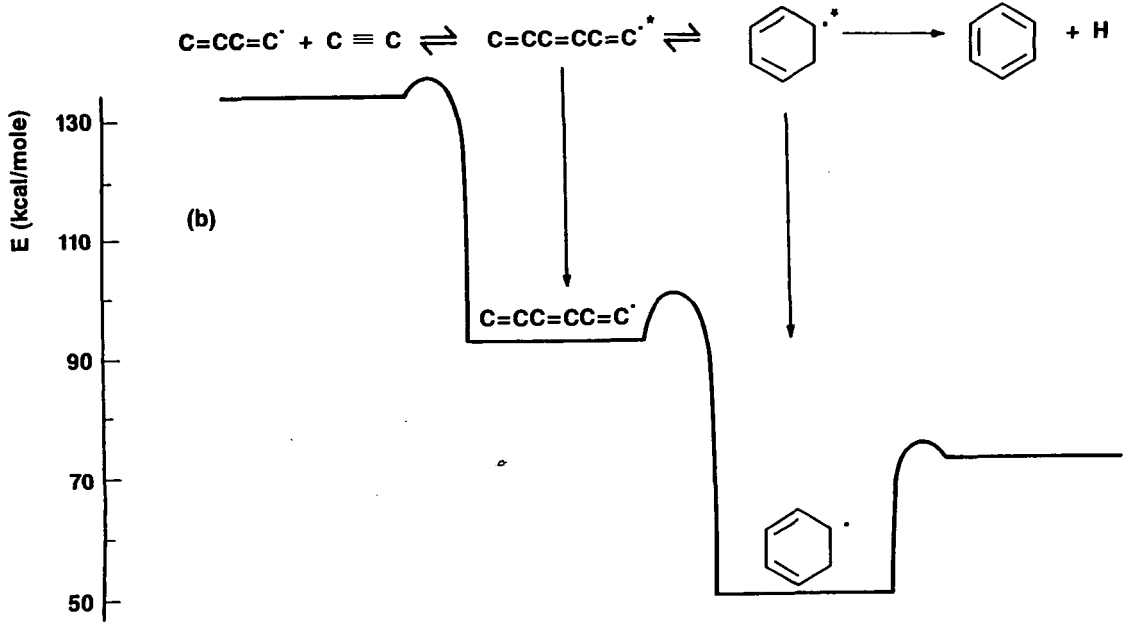

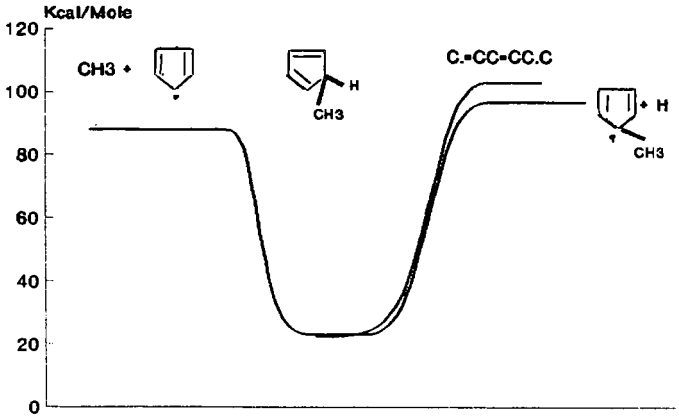
Kcal/Mole
120
100
80
60
40
20
0
CH3 •
H
CH3
C.=CC=CC.C
• H
CH3

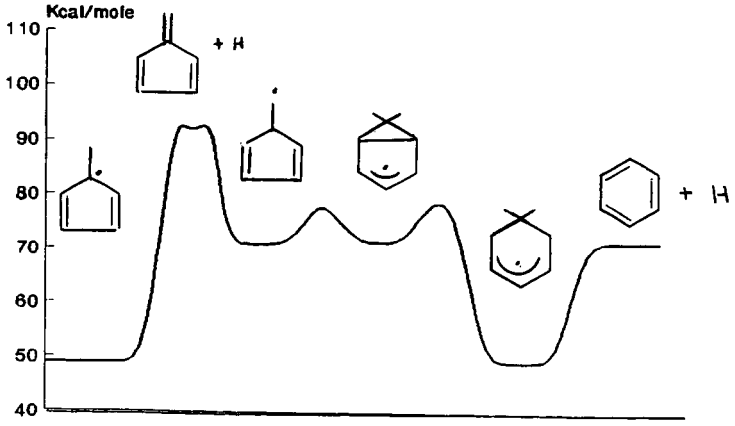
Kcal/mole
110
100
90
80
70
60
50
40
+ H
+ H

Figure 3

Figure 4

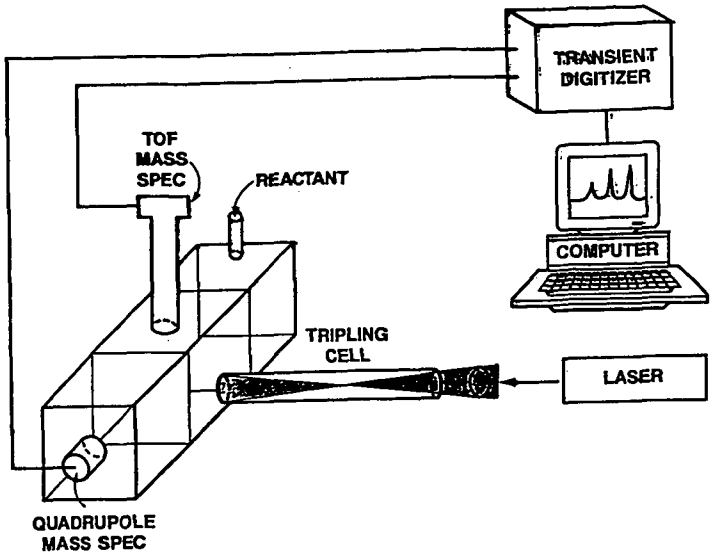
TRANSIENT DIGITIZER
TOF MASS SPEC
REACTANT
COMPUTER
TRIPLING CELL
LASER
QUADRUPOLE MASS SPEC

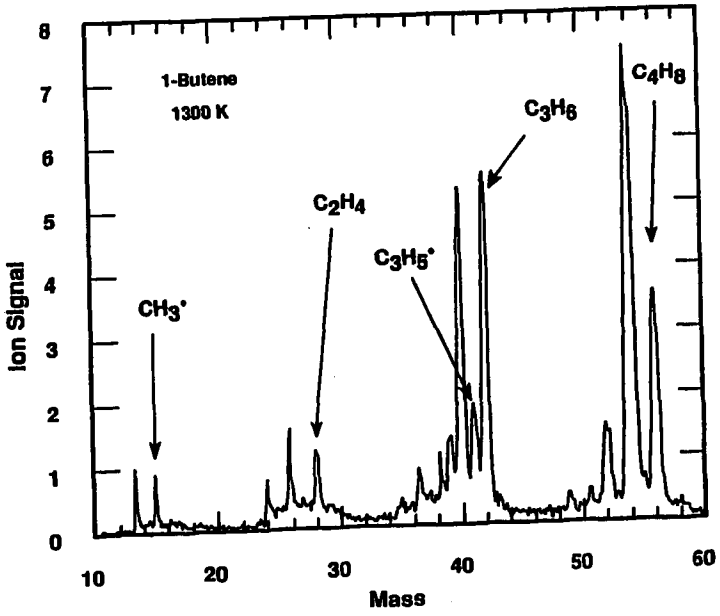
1-Butene
1300 K
$CH_3^•$
C_2H_4
$C_3H_5^•$
C_3H_6
C_4H_8
Ion Signal
Mass
0
1
2
3
4
5
6
7
8
10
20
30
40
50
60

Studies on The Reactions: $C_2H+C_2H_2 \rightarrow C_4H_2+H$ AND $C_2H+H_2 \rightarrow C_2H_2+H$

K. Fukuda, M. Koshi, and H. Matsui*
Department of Reaction Chemistry, The University of Tokyo
7-3-1 Hongo, Bunkyo-ku, Tokyo 113, Japan

Key Words: Reactions of Ethynyl Radical, Shock Tube, Flash Photolysis

1. Introduction

Ethynyl radical (C_2H) has been recognized as an important precursor of soot formation in the pyrolysis of acetylene and is also believed to be important in the formation of intersteller molecules. The rate constants of the elementary reactions of C_2H with C_2H_2 and H_2,

$$C_2H_2 + C_2H \rightarrow C_4H_2 + H \quad (1)$$

and

$$C_2H + H_2 \rightarrow C_2H_2 + H \quad (2)$$

have been measured by several groups at room temperature, however, some disagreement among them were indicated [1)-4)], also no direct data are available at high temperature range except for those based on indirect measurement on the pyrolysis of C_2H_2 [5)], or from speculative simulation [6)].

As the flash photolysis with intense excimer laser radiation combined with shock wave heating technique has enabled us to get direct information on the details of radical reactions at high temperature range, the processes (1) and (2) have been examined in this study. In addition, flash photolysis studies at room temperature with a mass spectrometer have been performed to ensure the temperature dependences on these reaction processes at wider temperature range. Thus, the kinetic informations derived in this work may be very useful both in the fundamentals of chemical kinetics as well as in the numerical simulations of practical combustion systems.

2. Experimental System

The details of the experimental systems were described in our previous publications [7),8)]. Two independent experimental systems have been used in this study: an excimer laser photolysis behind shock waves was used to study these reaction processes at elevated temperatures (above 1000 K), where, hydrogen atoms produced in the reactions were monitored by using atomic resonance absorption spectroscopy (ARAS), and an electron impact ionization mass spectroscopy was used to measure the rate constants and examine the reaction products at room temperature.

For the high temperature experiment, a diaphragmless shock tube of 5 cm i.d. made of stainless-steel was used. Sample gases were irradiated by an ArF laser (Questek V-β, about 15 ns pulse duration) through a rectangular quartz window (4cmx1cm) located at the end plate after being heated by reflected shock waves. C_2H_2 was photodissociated by the UV laser radiation to form C_2H and H. In the high temperature experiment, time dependence of H atoms produced in the photolysis (in the range of 10^{11}-10^{12}

molecules/cm^3) were monitored by an atomic resonance spectroscopic system (ARAS) at 121.6 nm. Absolute concentration of H atoms were decided by using a calibration curve which was decided by conducting thermal decomposition experiment using H_2-N_2O-Ar mixtures. The main advantage of the diaphragmless type shock tube is its excellent reproducibility of the shock heated condition: signal averaging at a fixed shock condition, when required, and plotting first-order rate against the concentration of the reacting partner in deciding the bimolecular rate constant were performed in this study to improve the quality of the kinetic informations.

The 193 nm photolysis experiemnt at room temperature was conducted in a slowly flowing pylex tube of 1.5 cm i.d. Sample gases were directly introduced into the vacuum chamber through a pinhole of 100μm i.d. and continuously detected by an electron-impact ionization mass spectrometer (Anelva TE 600-S).The ion signals froma secondary electron multiplier operated under pulse-counting conditions were recorded with a gated counter following pulse amplification and discrimination. Time dependence of the individual mass peak was obtained by scanning the delay time of the gate with the fixed gate width of 50 or 100 μs. Signals were averaged over 10^4 laser shots for each run.

3. Experimental Results

Firstly, the reactions of C_2H produced by an ArF laser photolysis in the mixtures of C_2H_2 and C_2H_2+H_2 highly diluted in Ar were studied behind reflected shock waves.
Typical oscillogram traces for the ARAS experiment behind shock waves are shown in Fig.3. The absorption intensity at 121.6 nm incresed when shock waves passed through the observation section due to C_2H_2. With a proper delay time (typically 50 μs) after the shock wave passage, ArF laser was fired and the rapid increment of the absorption intensity was observed by the production of H atoms by the photolysis of C_2H_2 : then, the intensity gradually increased to a steady state with a single-exponential profile.

The detailed mechanisms for the photodissociation of C_2H_2 by 193 nm laser has not been clarified yet. In this study, the rate of the incremnt of H atoms following the photolysis was not affected by the intensity of the ArF laser and, also the concentration of H atoms at steady state was always equal to about twice of that initially formed by the photolysis: moreover, the concentrations of the initial H atoms produced by the ArF laser photolysis was approximately proportional to the input laser energy, i.e., the ratio of (H) produced in the flash photolysis to the initial concentration of C_2H_2, $(H)/(C_2H_2)_0$ varied from about 0.15% to 1 % for the input laser powers of 10 to 60 mJ/cm^2 over the temperature range of 1000-2000 K. Thus, the multiphoton process that lead to the production of C_2+2H was concluded to be unimportant at this input energy range[9]. It was also confirmed that the rise rates of H atoms were proportional to both the initial concentration of C_2H_2 and that of added H_2, as are shown in Fig.4 and Fig.5.
Based on these experimental evidences, it was assumed that the

initial concentration of H atoms produced by the 193 nm photolysis was equal to that of $C_2H(X^2\Sigma^+)$ at the present experiment: the quenching rate of the possible electronically excited $C_2H(A^2\Pi)$ produced in the photolysis was supposed to be sufficiently fast in the time scale of the shock wave experiment. Thus, the informations on the time dependence of H atoms should be directly related to those for (1) or (2): the rate constants for these processes were evaluated from the slopes of the plot of the first order rate against initial concentrations of C_2H_2 and H_2 shown in Fig.4 and Fig.5, respectively.
The results are summarized as, $k_1 = (6.6\pm1.1)\times10^{-11}$ (cm^3 $molecule^{-1}$ s^{-1}) over T = 1260-2487 K without appreciable temperature dependence, and $k_2 = (3.3\times10^{-10})\exp(-13.8\ kcal\ mol^{-1}/RT)$ (cm^3 $molecule^{-1}s^{-1}$) over T = 1565-2218 K. In order to check the sensitivity of the side reactions in these experimental conditions, numerical computations including 11 elementary reactions were performed at some typical experimental runs; no effective contribution from the side reactions was found in evaluating k_1 and k_2.

The reaction processes (1) and (2) were examined by the 193 nm photolysis also at room temperature, where the time dependent concentration of C_4H_2 was monitored by an electron-impact mass spectrometer with an electron energy of 20 eV.

For the experiment on C_2H_2-Ar mixtures, as is shown in Fig.6, when C_2H_2 was irradiated by 193 nm, the concentration of C_4H_2 (m/e =50) increased exponentially towards steady level, and the rise rate of it linearly depended on the initial concentration of C_2H_2. From the slope shown in this figure, the rate constant was decided as, $k_1 = 4.6\times10^{-11}$ (cm^3 $molecule^{-1}s^{-1}$) at 293 K. This value is consistent with that at high temperature range.

When sufficient amount of H_2 was added to the C_2H_2-Ar mixtures, the rise rate of C_4H_2 became too large to decide the rate constant for (2) accurately. However, the experimental conditions were chosen so that the effect of the side reactions except (1) and (2) could be neglected (as was already noted avobe), then the reaction rate constant for (2) could be decided by measuring the steady state concentration of C_4H_2, $(C_4H_2)_\infty$ with the following relation,

$$(C_2H)_0/(C_4H_2)_\infty = 1 + (k_2/k_1)(H_2)/(C_2H_2) \qquad (3)$$

where, $(C_2H)_0$ is the initial concentration of C_2H produced by the ArF photolysis. Fig.7 shows the validity of this relation. The experiment was conducted with 0.63 and 0.74 Torr partial pressure of C_2H_2 and the energy of 193 nm laser was fixed to 12 mJ/cm^2, where, the pressure of H_2 was varied from 0 to 310 mTorr: the rate constant for (2) estimated from the slope of this plot was, $k_2 = 4.83\times10^{-14}$ (cm^3 $molecule^{-1}s^{-1}$) at 293 K.

4. Discussion and Comparison with The Previous Results

The present results on k_1 together with the previous ones are summarized in Fig.8. The present results agree well with that by Frank and Just[5] at high temperature range and also with those by Lange and Wagner[2] and Laufer and Bass[3] at room temperature: it is not clear why only the rate constant measured by Stephens et

al.[1] who monitored the concentration of C_2H by color centered laser was about 5 times faster than the previous studies[2,3] or present result. They attributed this differnce of the rate constants to the formation of the intermediate species, however, more direct evidence may be required to support this mechanism.

The other important reaction in the initiation stage of C_2H_2 pyrolysis (2) has been studied by several groups but the rate constant of it shows substantial disagreement each other[1)-4)]: the reaction intermediate was discussed in order to explain the difference between the rate of reactant and products. As can be seen in Fig.9, the present result on k_2 at room temperature was smaller than the previous ones. This process is supposed to have substantial temperature dependence because of the energy barrier of the transition state. No direct experimental data at high temperature are available, although some speculative rate constant has been used in the computer simulations[5)]. The rate constant suggested in the previous works has shown highly non-Arrhenius temperature dependence. Our results at high temperature range has considarably large temperature dependence, thus, the extrapolation of them to the room temperature range gives much smaller rate constant than those directly measured. Such non-Arrhemius temperature dependence of the rate constant for (2) was discussed by Harding et al. based on transition state properties of C_2H estimated by ab initio calculation[10)]. Although the observed activation energy in this study (13.8 kcal/mol) was much larger than that estimated in POL-CI calculation (4.0 kcal/mol), the TST theory seems consistent with the present experiment: it is suggested that the large temperature dependence of the rate constant for (2) was brought both by the temperature dependence of vibrational partition function of the transition state (high temperature range) and tunneling effect (low temperature range).

References

1. J.W. Stephens, J.L. Hall, H. Solka, W.B. Yan, R.W. Curl, G.P. Glass, J. Chem. Phys., 91 5740 (1987)
2. W. Lange and H.G. Wagner, Ber. Bunsenges. Phys. Chem., 79 165 (1975)
3. A.H. Laufer and A.M. Bass, J. Phys. Chem., 83, 310 (1979)
4. A.M. Renlund, F. Shokoohi, H. Reisler, and C. Wittig, Chem. Phys. Lett., 84 293 (1981)
5. P. Frank and Th. Just, Comb. Flame 38 231 (1980)
6. W. Tsang and R.F. Hampson, J. Phys. Chem. Ref. Data, 15 1087 (1986)
7. M. Koshi, M. Yoshimura, K. Fukuda, and H. Matsui, J. Chem. Phys., 93 8703 (1990)
8. M. Koshi, A. Miyoshi, and H. Matsui, Chem. Phys. Lett. (under submission)
9. T.A. Cool, P.M. Goodwin, and C.E. Otis, J. Chem. Phys., 93 3714 (1990)
10. L.B. Harding, G.C. Schatz, and R.A. Chiles, J. Chem. Phys.,76 5172 (1982)

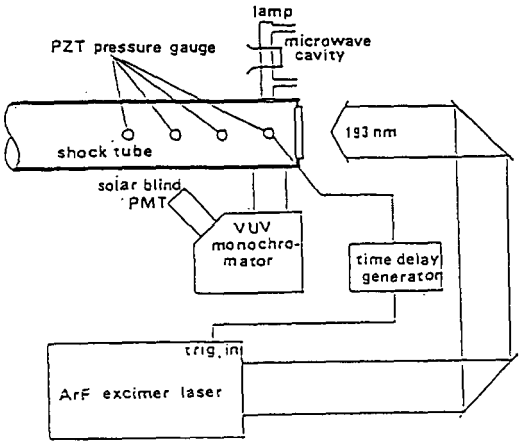

Fig.1 A schematic of the shock tube - laser flash photolysis system used in the high temperature experiment

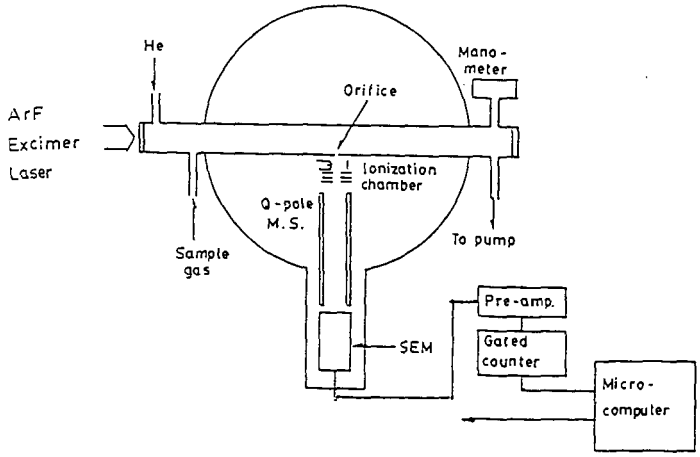

Fig.2 A schematic of the laser photolysis - mass specrometer system used in the room temperature experiment

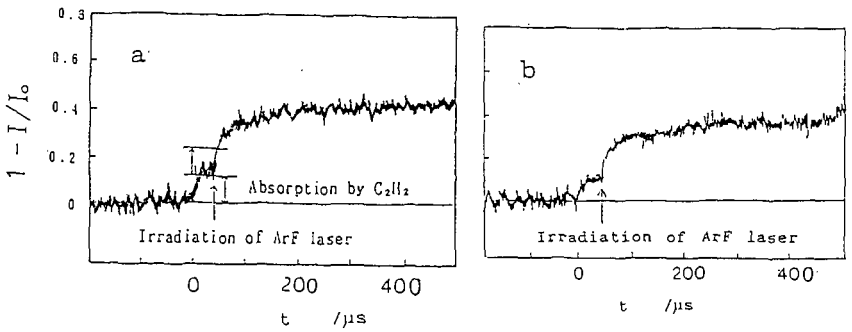

Fig.3 Examples of oscillogram trace of 121.6 nm absorption in ArF photolysis behind reflected shock waves
a: 86 ppm C_2H_2 in Ar, T = 1758 K, p = 1.92 atm.
b: 21 ppm C_2H_2 + 400 ppm H_2 in Ar, T = 1639 K, p = 1.33 atm.

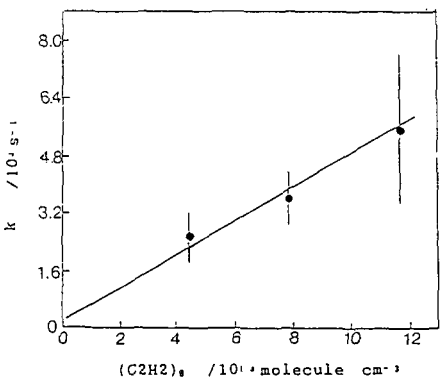

Fig.4 Dependence of the rate of increment of H atoms on the initial concentration of C_2H_2 (T = 1640 ± 20 K, p_1 = 20 Torr, 30-150 ppm C_2H_2 diluted in Ar)

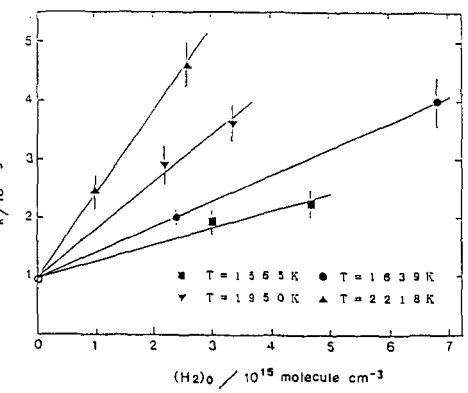

Fig.5 Dependence of the rate of increment of H atoms on the initial concentration of H_2 (21 ppm C_2H_2 +400-1100 ppm H_2 diluted in Ar, p_1 =20 Torr)

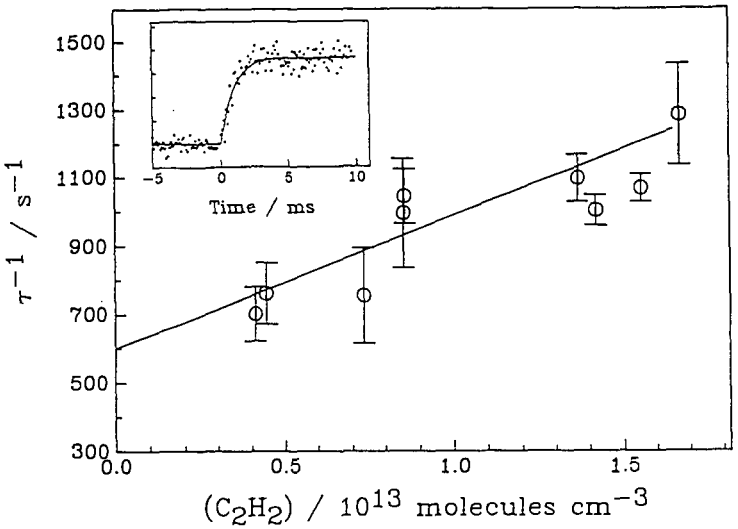

Fig.6 First order production rates of C_4H_2 as a function of C_2H_2 concentrations. A time profile shown in the figure was taken with $(C_2H_2)0=8.6\times10^{12}$ molecules/cm^3.

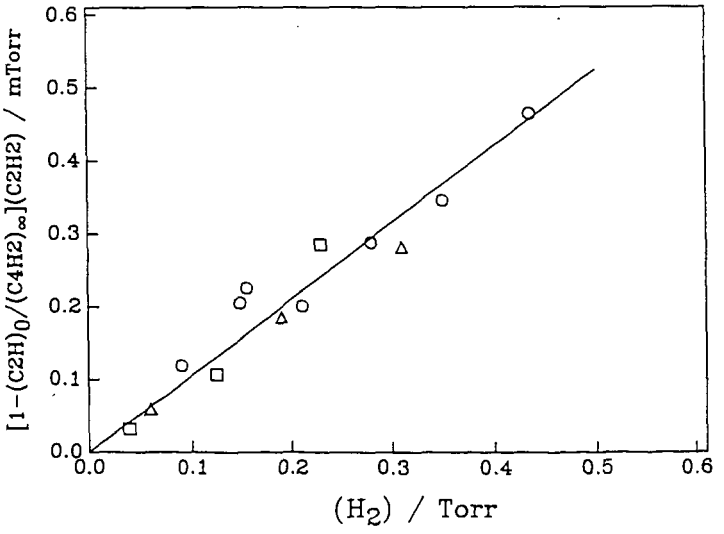

Fig.7 Plot of $[1-(C_2H)_0/(C_4H_2)_\infty](C_2H_2)$ vs (H_2). Slope of this plot is equal to k_2/k_1 (see Eq.(3)). ○;(C_2H_2)=0.24 mTorr, □;(C_2H_2)=0.63 mTorr, △;(C_2H_2)=0.74 mTorr.

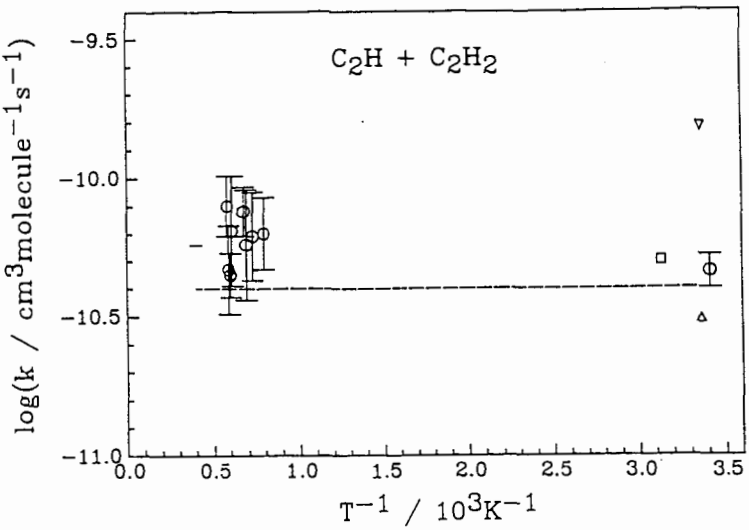

Fig.8 Arrhenius plot for the rate constant of the $C_2H+C_2H_2 \rightarrow C_4H_2+H$ reaction. ⊕;This work, ▽;ref.1, □;ref.2, △;ref.3, —;ref.5, – –;ref.6.

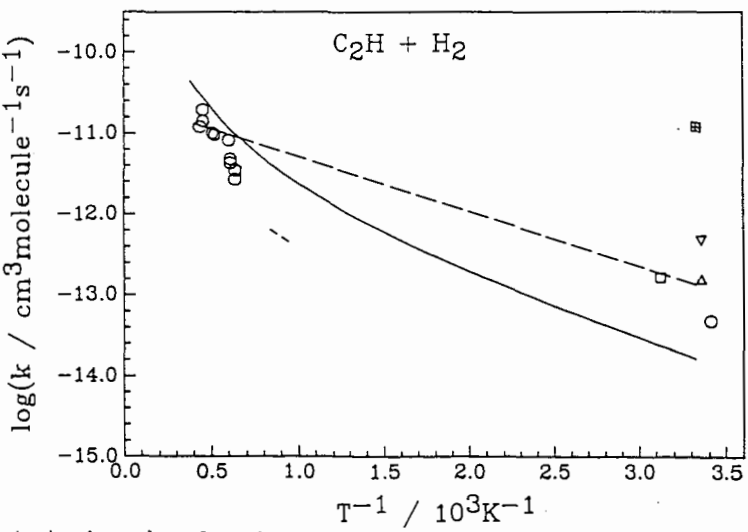

Fig.9 Arrhenius plot for the rate constant of the $C_2H+H_2 \rightarrow C_2H_2+H$ reaction. ○;This work, ▽;ref.1, □;ref.2, △;ref.3, ⊞;ref.4, – –;ref.6. A solid curve is a result of TST calculation with parameters given in ref.10.

QUENCHING OF DIACETYLENE FORMATION DURING THE REACTION OF OXYGEN ATOMS WITH ACETYLENE AT 300 K

David E. Phippen and Kyle D. Bayes
Department of Chemistry and Biochemistry
University of California, Los Angeles, CA 90024-1569

KEYWORDS: diacetylene, acetylene, oxygen atoms

ABSTRACT

The production of diacetylene in the low pressure reaction of oxygen atoms with acetylene was monitored with a photoionization mass spectrometer. The addition of methane, nitrous oxide or molecular hydrogen quenched the formation of diacetylene. Stern-Volmer kinetics were observed, which implies that both acetylene and the quenching gas compete for a single reactive intermediate. This quenching appears to be closely connected with the quenching of chemi-ionization reported previously (*Chem. Phys. Lett.* **164**, 625(1989)). Quantitative comparisons of quenching rates with known rate constants suggest that $CH(X^2\pi)$ is the intermediate involved. Application of an electric field to this system had no affect on the diacetylene concentration, showing that chemi-ions are not involved in C_4H_2 formation.

INTRODUCTION

Diacetylene (C_4H_2) is an important intermediate in the combustion of acetylene and other hydrocarbons, especially for fuel-rich conditions [1-5]. As much as 35% of the acetylene consumed in a flame may pass through C_4H_2 [4]. It has been argued that diacetylene and heavier polyacetylenes are precursors of soot [1,4], although others do not support this proposal.

The atomic oxygen-acteylene system has been studied extensively and there is agreement that the mechanism of diacetylene formation is complex [6-8]. The initial rate of formation of C_4H_2 is proportional to the product of concentrations $[O][C_2H_2]$, and this rate can be accelerated by adding hydrogen atoms or inhibited by adding O_2 or H_2.

The reaction that forms diacetylene in flames has not been clearly established. The reaction usually proposed is,

$$C_2H + C_2H_2 \longrightarrow C_4H_2 + H \qquad (1)$$

and this reaction is known to be fast [9]. However, a reasonable source of C_2H radicals in flames is not known. The direct abstraction, favored in the past,

$$O + C_2H_2 \longrightarrow C_2H + OH \qquad (2)$$

is now known to be endoergic by 30 kcal mol^{-1} [10], and thus can be ignored except for very high temperature combustion.

We have extended earlier quenching studies [11] in an attempt to clarify the mechanisn by which diacetylene is formed during acetylene combustion.

EXPERIMENTS

Oxygen atoms were made by discharging a flowing mixture of 0.5% CO_2 in He in a microwave discharge (2450 MHz). Titration with NO_2 showed that the typical [O] was 3 mTorr. Acetylene, also diluted in He, and other quenching gases were added upstream of the pinhole to a photoionization mass spectrometer. The diacetylene was photoionized by Lyman α radiation (10.2 eV) and detected at mass 50. The total pressure was kept constant at 3 Torr as the quenching gases were added by varying the He flow. Further experimental details are given elsewhere [12].

RESULTS and DISCUSSION

We have observed that adding methane, nitrous oxide or molecular hydrogen to the O + C_2H_2 system quenches the formation of diacetylene. These quenching molecules are relatively inert to attack by oxygen atoms at 300 K for the short contact times (<15 ms) used in this study.

For methane and nitrous oxide the quenching followed a simple Stern-Volmer law, as can be seen in Figure 1. The quenching efficiency depends on the partial pressure of acetylene present. The original data are recorded elsewhere [12].

Simple Stern-Volmer plots suggest that both acetylene and the quencher molecule are competing for the same intermediate. If the intermediate, I, reacts with acetylene, a molecule of diacetylene is formed (not necessarily in a single step).

$$I + C_2H_2 \longrightarrow \longrightarrow C_4H_2 \qquad (3)$$

$$I + Q \longrightarrow \text{other products} \qquad (4)$$

$$I \longrightarrow \text{other products} \qquad (5)$$

Reaction between I and quencher molecule Q does not result in diacetylene formation. Reaction (5) is included to allow loss of I by other reactions, on the walls, etc.

If it is assumed that the addition of Q does not affect the rate of formation of I, then reactions 3, 4 and 5 lead to the steady state expression,

$$\frac{[C_4H_2]_o}{[C_4H_2]} = 1 + \frac{k_4[Q]}{k_3[C_2H_2] + k_5} \qquad (A)$$

where $[C_4H_2]_o$ refers to the diacetylene signal when no quencher gas is present. The quenching data for methane and nitrous oxide have been fit to Equation A using least squares.

If Equation A is valid, the inverse of the slopes of the Stern-Volmer plots should depend linearly on the acetylene concentration. A test of this relationship is shown in Figure 2. For this simple model, the slopes of the lines in Figure 2 then give the ratios for k_3/k_4 and the intercepts give k_5/k_4. Values for these k_3/k_4

ratios are collected in Table I.

Molecular hydrogen was a less efficient quencher than methane or nitrous oxide and so more of it was necessary to give significant quenching. The resulting Stern-Volmer plots were slightly concave downward. It is not clear if this indicates that a more complex quenching mechanism is needed, or that some other effect resulting from the large concentrations of H_2 is involved. It is known that hydrogen atoms promote the formation of diacetylene [8], and it is possible that the large H_2 concentrations could result in hydrogen atoms being produced (e.g. by collisional dissociation of H_2 by $CO(a^3\pi)$, which is produced in this system [13], or by radical attack on H_2). The hydrogen quenching curves could be fit to equations of the form,

$$\frac{[C_4H_2]_o}{[C_4H_2]} = 1 + \beta[H_2] + \gamma[H_2]^2 \qquad (B)$$

By analogy to Eqn. A, the reciprocal of β was plotted against the acetylene concentration, and the resulting points are consistent with a straight line (Fig. 2). The slope of this line is entered in Table 1 under k_3/k_4 for hydrogen with the understanding that this assignment is tentative.

The second column of numbers in Table 1 gives the ratio of k_3/k_4 if the intermediate I is the ground state C_2H radical. According to the present study, the precursor to diacetylene reacts with methane only 2.7 times slower that it does with acetylene, while C_2H reacts 50 times slower. The tentative ratio for hydrogen is also not compatible with the intermediate being C_2H. Unfortunately, the rate constant for C_2H reacting with N_2O has not been measured yet. From the comparison of the first two columns of Table I, we conclude that the intermediate I is not the C_2H radical.

The CH radical has been proposed by Homann and Schweinfurth as one of the precursors leading to diacetylene [8]. The third column of Table I gives the ratios of k_3/k_4 for $CH(X^2\pi)$. In comparing the first and third columns of Table I, better agreement is seen, although the values for hydrogen still differ significantly.

A more impressive comparison can be made between the quenching of chemi-ionization reported previously for this system [11] and the quenching of diacetylene. The fraction of the chemi-ionization that can be quenched follows a Stern-Volmer law, and a plot of the reciprocal of the Stern-Volmer slopes vs. acetylene looks very similar to the present Figure 2. In particular, for methane quenching, the lines show identical slopes, i.e. identical values for k_3/k_4. Quenching by N_2O also agrees closely ($k_3/k_4 = 3.5$ for chemi-ionization quenching, compared to 4.8 in Table I). Since the quenching of the chemi-ionization almost certainly involves reaction with the $CH(X^2\pi)$ radical, this strengthens the case for CH being a precursor to diacetylene.

The similarity of quenching of chemi-ions and diacetylene raises the possibility that chemi-ions might be precursors to diacetylene. This possibility was tested in a radial electric field reactor, with a pinhole leading to the photoionization mass spectrometer. The diacetylene signals with and without an electric field (4.8 Townsend)

were carefully compared; no change in intensity could be observed (<5%). The smaller peak at mass 52 (C_4H_4) also did not change. Since this electric field will reduce the residence time of the chemi-ions by approximaetly a factor of 100, we must conclude that chemi-ions are not precursors to the observed diacetylene in this system.

In the Homann and Schweinfurth mechanism [8], the CH radical reacts with acetylene to form C_3H_2, which subsequently reacts with an oxygen atom to form C_2H. The diacetylene is then formed when C_2H reacts with another acetylene (Reaction 1). If this were the correct mechanism, then adding a quenching molecule that could react with both CH and C_2H should give Stern-Volmer plots that curve upward. The magnitude of this effect can be seen in Figure 3, where the solid curves show the expected behavior for methane quenching using known rate constants for C_2H and a linear term that fits the initial slope. The lack of curvature in the experimental points suggests that sequential quenching of two precursors is not important for this system.

If $CH(X^2\pi)$ is the radical that is being intercepted by the various quenching molecules, then it is very likely that the reaction,

$$CH(X^2\pi) + C_2H_2 \longrightarrow C_3H_2 + H \qquad (6)$$

is the next step in forming diacetylene. Reaction 6 is sufficiently exoergic to form any one of the three isomers of C_3H_2. Direct sampling and trapping studies have shown evidence for C_3H_2 in flames [3,14]. However, very little is known about the kinetic behavior of any of these isomers. The mechanism leading from C_3H_2 to diacetylene can only be speculative at this time. However, it should be noted that any of the following intermediates that are known to be present in this system could donate a carbon atom to C_3H_2 to give diacetylene in an exoergic reaction: C; C_2O; CH; vinyledene; CH_2; HC_2O; or C_3H_2 itself.

CONCLUSIONS

The present quenching studies, especially the results with methane which are the most extensive, do not support C_2H as the precursor to diacetylene in the oxygen atom-acetylene system. Combining the present results with those from a previous chemi-ion quenching study suggests that $CH(X^2\pi)$ is the intermediate that is being quenched. Quenching by molecular hydrogen is anomalous and is not understood. Clearly chemi-ions do not participate in the formation of diacetylene. Kinetic studies need to be done on the C_3H_2 isomers to understand the next step in the formation of diacetylene in this system.

REFERENCES

[1] K. H. Homann and H. Gg. Wagner, *Ber. Bunsenges. Phys. Chemie* **69**, 20 (1965).
[2] J. Warnatz, H. Bockhorn, A. Moser and H. W. Wenz, *Symp. (Int.) on Combust. [Proc.], 19th*, 197 (1982).
[3] J. D. Bittner and J. B. Howard, *Symp. (Int.) on Combust. [Proc.], 19th*, 211 (1982).
[4] J. Warnatz, *Comb. Sci. Technol.* **26**, 203 (1982).
[5] H. G. Wagner and B. S. Haynes, *Prog. Energy Combust. Sci.*, **7**, 229 (1981).
[6] I. T. N. Jones and K. D. Bayes, *Symp. (Int.) on Combust. [Proc.], 14th*, 277 (1973).
[7] K. H. Homann, J. Warnatz and C. Wellmann, *Symp. (Int.) on Combust. [Proc.], 16th*, 853 (1977).
[8] K. H. Homann and H. Schweinfurth, *Ber. Bunsenges. Phys. Chemie* **85**, 569 (1981).
[9] J. W. Stephens, J. L. Hall, H. Solka, W. B. Yan, R. F. Curl and G. P. Glass, *J. Phys. Chem.* **91**, 5740 (1987).
[10] B. Ruscic and J. Berkowitz, *J. Chem. Phys.* **93**, 5586 (1990).
[11] D. E. Phippen and K. D. Bayes, *Chem. Phys. Lett.* **164**, 625 (1989).
[12] D. E. Phippen, Ph.D. thesis, University of California, Los Angeles, 1991.
[13] K. H. Becker and K. D. Bayes, *J. Chem. Phys.* **48**, 653 (1968).
[14] M. Hausmann and K. H. Homann, *Ber. Bunsenges. Phys. Chemie* **94**, 1308 (1990).

Table I: Comparison of Experimental Ratios of k_3/k_4 with Ratios of Known Rate Constants. Rate constants for C_2H were taken from [9] and from Lander *et al.* (*J. Phys. Chem.* **94**, 7759 (1990)). Rate constants for $CH(X^2\pi)$ were taken from the review by Sanders and Lim (*Chemical Kinetics of Small Organic Radicals*, Vol. 3, ed. Z. Alfassi, CRC Press, Boca Raton, 1986, p. 103). 95% confidence limits for k_3/k_4 are shown.

Quencher	Experimental k_3/k_4	If intermediate is C_2H	If intermediate is $CH(X^2\pi)$
CH_4	2.7 ± 0.5	50	4.1
N_2O	4.8 ± 0.9	?	5.4
H_2	17 ± 7	340	>400

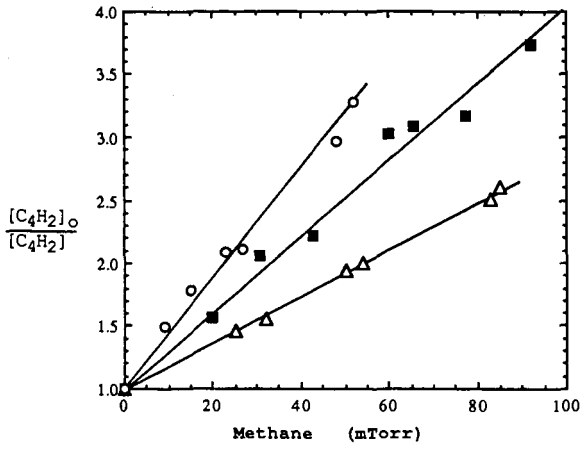

Figure 1: Stern-Volmer Plot of Diacetylene Quenching by Methane. The different symbols represent different partial pressures of acetylene: circles 3.9 mTorr; squares 8.4 mTorr; triangles 14 mTorr. All runs had [O] of 2.7 mTorr and 3 Torr total pressure. The least squares lines were forced through unity at zero methane.

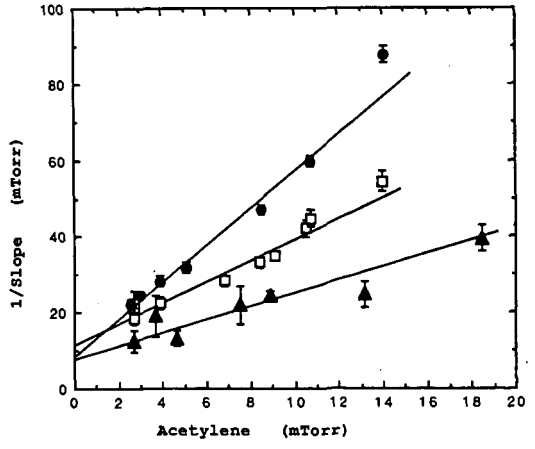

Figure 2: Reciprocal of the Stern-Volmer Slopes as a Function of Acetylene. The solid circles represent quenching by methane and the open squares quenching by nitrous oxide. For hydrogen the values of β^{-1} have been divided by 10 before being plotted. The straight lines represent weighted least squares calculations. The slopes of these lines are entered in the first column of Table I.

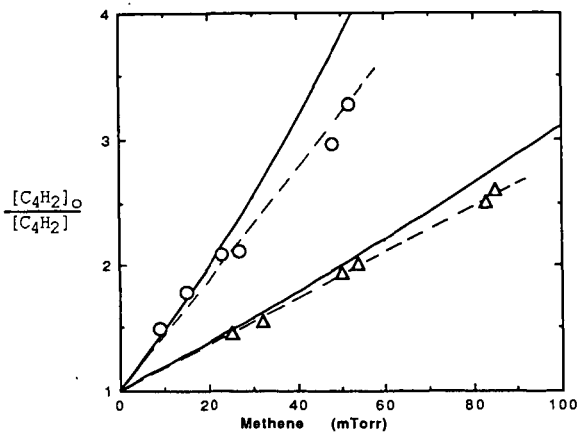

Figure 3: Comparison of Observed Quenching Data with Model for Sequential Quenching. Data are the same as in Figure 1.

KINETICS AND THERMOCHEMISTRY OF THE OXIDATION OF UNSATURATED RADICALS: n-C_4H_5 + O_2

D. Gutman, I. R. Slagle, A. Bencsura, and S.-B. Xing
Department of Chemistry
Catholic University of America
Washington, DC 20064

Keywords: unsaturated radicals; C_4H_5 + O_2; C_4H_5 + C_2H_2

INTRODUCTION

The reactions of unsaturated free radicals (such as C_3H_3 and C_4H_5) either with themselves or with small unsaturated molecules have been proposed as pathways leading to the eventual formation of aromatic compounds and soot.[1] Little is known about the reactions of these intermediates. In particular, the chemistry of the butadienyl radical (C_4H_5) is almost completely unknown. In order to test the feasibility of this radical as a soot precursor, it is important to determine if molecular oxygen can compete as a radical sink for C_4H_5 in combustion systems, preventing the growth of [C_4H_5] to levels where reactions producing aromatic compounds can occur at a measurable rate. In this paper we report a direct experimental study of the kinetics and thermochemistry of the reaction of C_4H_5 with O_2 and use the results obtained to infer some general mechanistic pathways for the reactions of hydrogen-deficient free radicals with molecular oxygen.

EXPERIMENTAL

Apparatus and General Procedure Details of the experimental apparatus and procedures have been published elsewhere[2] and only those aspects of the method which are unique to the present study will be described in detail here. Pulsed, unfocused 193-nm or 248-nm radiation (≈5 Hz) from a Lambda Physik EMG 201 MSC excimer laser was directed along the axis of a heatable, boric acid-coated quartz reactor (1.05-cm-i.d.). Gas flowing through the tube at ≈4 m s^{-1} contained the butadienyl radical precursor (trans-1,3-pentadiene) in small amounts, oxygen, and helium. The flowing gas was completely replaced between laser pulses. Gas was sampled through a hole (0.043-cm diameter) located at the end of a nozzle in the side of the reactor and formed into a beam by a conical skimmer before the gas entered the vacuum chamber containing the photoionization mass spectrometer (PIMS). As the gas beam traversed the ion source, a portion was photoionized using resonance lamps (10.2 and 8.9-9.1 eV) and mass selected. Temporal ion signal profiles of the reactant radical, products and the radical precursor were recorded on a multichannel scalar from a short time before each laser pulse up to 20 ms following the pulse. Data from 1000 to 45,000 repetitions of the experiment were accumulated before the data were analyzed.

Photolysis of Butadienyl Radical Precursors and the Nature of the C_4H_5 Radical A survey was conducted to determine the products of the photolysis of two possible C_4H_5 radical precursors: trans-1,3-pentadiene (expected to produce the 1-butadienyl radical) and 2-methyl-1,3-butadiene (expected to produce the 2-butadienyl radical). This survey was conducted at two photolysis wavelengths (193 and 248 nm) and two temperatures (298 and 650K). The mass spectrometric results were essentially the same at both wavelengths, with either precursor, and at either temperature. The largest ion signal detected after photolysis corresponded to the mass of C_5H_6, a stable product. Smaller signals of approximately equal amplitude were detected at the mass numbers corresponding to C_4H_5, C_3H_5, C_3H_3 and C_5H_7. These ion signals exhibited the temporal behavior of free radicals with the signals decaying in an exponential manner due to the presence of heterogeneous wall effects. Smaller amounts of CH_3, C_2H_3, C_2H_5, C_3H_6, and C_4H_4 were also detected. These results indicate that the important photolysis routes are

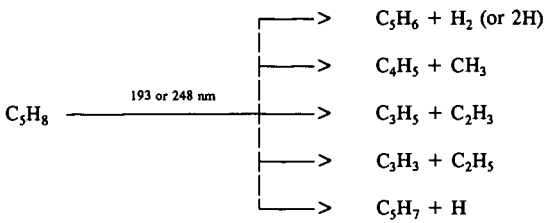

While PIMS is a sensitive method for detecting small concentrations of free radicals (even in the presence of large concentrations of radical precursors), it cannot distinguish between structural isomers unless the ionization potentials of these isomers are extremely different. Such is not the case for the C_4H_5 isomers. However, it is likely that the initial photolysis occurs at different sites in the two C_5H_8 compounds studied here with the 1,3-pentadiene producing the 1-butadienyl radical,

$$CH_3\text{-}CH{=}CH\text{-}CH{=}CH_2 \longrightarrow \cdot CH{=}CH\text{-}CH{=}CH_2 + CH_3$$

while the 2-methyl-1,3-butadiene produces the more stable 2-butadienyl radical.

$$CH_2{=}C(CH_3)\text{-}CH{=}CH_2 \longrightarrow CH_2{=}\dot{C}\text{-}CH{=}CH_2 + CH_3$$

Although PIMS cannot distinguish between these two structural forms (or between a third form common to both precursors), a difference in observed reactivity can indicate the presence of two distinct isomers. At very low initial concentrations where radical-radical reactions are unimportant and in the absence of any other reactants, both possible C_4H_5 species react in a similar manner, displaying a simple exponential decay due to the presence of heterogeneous effects. However, when molecular oxygen is added to the system, there is a distinct difference in the temporal behavior of the two species. At room temperature in the presence of added oxygen the C_4H_5 produced from the pentadiene reacts slowly and decays in a purely exponential manner. On the other hand, the C_4H_5 from the methylbutadiene reacts much more rapidly with a temporal behavior that is bi-exponential (perhaps indicating the presence of two structural forms of C_4H_5 with very different reactivities). At higher temperatures in the presence of oxygen, the temporal ion signal profiles of both species exhibit bi-exponential behavior but with extremely different time constants, the C_4H_5 from the methylbutadiene always decaying much more rapidly than that from the pentadiene. On the basis of this difference in reactivity we conclude that the C_4H_5 produced from the 1,3-pentadiene is indeed the 1-butadienyl radical.

Measurement of $C_4H_5 + O_2$ Reaction Rate Parameters In the experiments reported here the 1-butadienyl radical was produced in presence of varying amounts of oxygen by the 193- or 248-nm photolysis of 1,3-pentadiene. Initial radical concentrations were chosen to be low enough to ensure that radical-radical recombination reactions, either of C_4H_5 with itself or with the other products of the photolysis, had negligible rates compared to the reaction of interest. The absence of radical-radical reactions was confirmed at each set of experimental conditions reported here by varying the initial pentadiene precursor concentration. These tests also confirmed that the reaction of C_4H_5 with C_5H_8 had a negligible rate under these conditions. Reaction rate parameters were also found to be independent of laser wavelength and intensity. These tests ensure that the 1-$C_4H_5 + O_2$ reaction was in fact isolated for direct study.

Search for Products of the $C_4H_5 + O_2$ Reaction The search for possible products of the $C_4H_5 + O_2$ reaction was hampered by the production of the additional C_5H_8 photolysis products, the low concentrations of C_4H_5 radicals necessary to avoid recombination reactions, and the high oxygen concentrations used in this study. The photolysis of pentadiene produces many radicals which are themselves possible products of the $C_4H_5 + O_2$ reaction or which react more rapidly with O_2 than C_4H_5 to produce the same possible products. For example, C_4H_4, a stable photolysis product, is also the product expected from either the direct abstraction of a hydrogen atom from C_4H_5 by O_2 or by the subsequent decomposition of a $C_4H_5O_2$ adduct. Another photolysis product, C_2H_3, reacts rapidly

with O_2 to produce H_2CO while $C_3H_3 + O_2$ produces ketene at high temperatures. The $C_4H_5O_2$ adduct itself could not be detected. This was not unexpected since alkylperoxy radicals are not readily detected by PIMS. Another possible product, C_4H_4O, could not be detected because it lies at the same mass number as the precursor molecule. C_3H_4O, a product analogous to the ketene produced in the high-temperature $C_3H_3 + O_2$ reaction, was observed at 900K, but could not be confirmed as a product of the $C_4H_5 + O_2$ reaction since its temporal behavior did not mirror that of the C_4H_5 radical. There were no product signals detected that could be unambiguously assigned to the $C_4H_5 + O_2$ reaction. Since the mechanism for this reaction could not be established by direct methods, it will be assigned based on rate data and using analogies with what is known about the mechanisms of the reactions of similar unsaturated radicals.

RESULTS

From a preliminary set of experiments conducted over the temperature range of this study (295 - 900K), it was discovered that the 1-$C_4H_5 + O_2$ reaction has different mechanisms at low and high temperatures and that at intermediate temperatures (369 - 409K at the oxygen pressures used in these experiments) the equilibrium

$$C_4H_5 + O_2 (+M) \rightleftharpoons C_4H_5O_2 (+M) \qquad (1)$$

is clearly established.

The results obtained will be discussed separately for the three temperature ranges in which different kinetic behavior was observed. Rate constants were measured at three densities at room temperature and at two densities in the high temperature region. Equilibrium constants for reaction 1 were determined in the intermediate region. The conditions of all these experiments and the results obtained are given in Table I and plotted in Figures 1 and 2.

Room Temperature Reaction Near room temperature the $C_4H_5 + O_2$ reaction proceeds by simple addition

$$C_4H_5 + O_2 \longrightarrow C_4H_5O_2 \qquad (1)$$

The temporal behavior of C_4H_5 in the presence of an excess of O_2 can be characterized by a simple first-order decay, with a decay constant (k') equal to the sum of $k_1[O_2]$ and k_2 where k_2 is the rate for the heterogeneous loss of C_4H_5.

$$C_4H_5 \longrightarrow \text{Heterogeneous loss} \qquad (2)$$

The bimolecular rate constant was obtained from the slope of the line fitted through the measured decay constants plotted against $[O_2]$. From the density dependence of this rate constant $(\Delta \log (k)/\Delta \log [M]) \approx 0.4$, it is apparent that the reaction is near the middle of the fall-off region at the densities used in this study ($6\text{-}18 \times 10^{16}$ molecule cm^{-3}). (See Figure 1.) The addition mechanism is inferred from this density dependence of the rate constant as well as the fact that the reaction is reversible at higher temperatures.

Intermediate Temperature Range Between 369 and 409K the loss of C_4H_5 in the presence of O_2 was not a simple exponential decay but was rather a rapid decay followed by a much slower one which is characteristic of the radical reaching an observable equilibrium with O_2, reaction 1. The second, slower decay is due to competing processes, such as the heterogeneous removal of C_4H_5 at the walls (reaction 2), other possible reactions of C_4H_5 with O_2, or other reactions of $C_4H_5O_2$ that produce products other than the original reactants. As can be seen in Table Ib, this second decay constant, m_2, increases with temperature while the wall loss rate (reaction 2) remains essentially constant. This observation indicates that a change in reaction mechanism is occurring in this temperature range. This conclusion is supported by the fact that an observable reaction of C_4H_5 with O_2 continues to occur at higher temperatures (see below), where normally equilibrium of C_4H_5 and $C_4H_5O_2$ would be established before measurable amounts of C_4H_5 had reacted with O_2.

The equilibrium constant, K_1, was obtained from the parameters of the double exponential function[3] which was fit to the experimental C_4H_5 ion signal profiles in this temperature range. The relationship between K_1 and these parameters is determined by the mechanism responsible for the temporal behavior of the C_4H_5. From the presence of a high temperature reaction and by analogy with reactions of other radicals, such as ethyl and propargyl, which exhibit similar behavior, we

conclude that the $C_4H_5 + O_2$ mechanism involves three steps: reversible addition (reaction 1), heterogeneous loss of C_4H_5 (reaction 2) and the unimolecular decomposition of the $C_4H_5O_2$ adduct.

$$C_4H_5O_2 \longrightarrow \text{Products} \quad (3)$$

Thermodynamic functions for reaction 1 were obtained from the temperature dependence of K_1[2]. The values of ΔH°_{298} and ΔS°_{298} were determined from the slope and the intercept of the straight line fitted through the measured equilibrium constants on a modified van't Hoff plot (see Figure 2). They are

$$\Delta H^\circ_{298} = -18.7 \pm 0.8 \text{ kcal mol}^{-1}$$
$$\Delta S^\circ_{298} = -29.8 \pm 2.2 \text{ cal mol}^{-1} \text{ K}^{-1}$$

The correction to the ordinate variable, ln K_P, on the modified van't Hoff plot (which converts $-\Delta G^\circ_T/RT$ to $-\Delta G^\circ_{298}/RT$) is small (0.7 to 2%) and is obtained from heat capacities estimated by using group-additivity rules.

High Temperature Reaction (600 - 900K) Above the temperature at which equilibrium can be observed, C_4H_5 continues to react with O_2. Radical decay profiles in this temperature region are again simple exponential functions and the decay constants (k') are proportional to $[O_2]$. The phenomenological bimolecular rate constants are independent of a factor of two in density (6 - 12×10^{16} molecule cm^{-3}) and increase with temperature in this regime (see Figure 1). The bimolecular rate constants for the overall reaction

$$C_4H_5 + O_2 \longrightarrow \text{Products} \quad (4)$$

were obtained in the same manner as for the low temperature reaction, i.e., from the slope of the line fitted through the measured first order decay constants plotted against $[O_2]$, and were fit to an Arrhenius expression

$$k_4 = 6.9 \times 10^{-14} \exp(-2.5 \text{ kcal mol}^{-1}/RT) \text{ cm}^3 \text{ molecule}^{-1} \text{ s}^{-1}$$

In the high temperature region the bimolecular rate constant increases with temperature and has no systematic density dependence. These observations indicate the importance of an irreversible $C_4H_5 + O_2$ reaction path at elevated temperatures which proceeds over an energy barrier.

$C_4H_5 + C_2H_2$ Reaction An attempt was made to observe a possible reaction of C_4H_5 with acetylene at 950K, a reaction indicated as potentially important in the formation of aromatic compounds.[1] There was no increase in the C_4H_5 decay rate over the heterogeneous loss rate when 3×10^{15} molecule cm^{-3} of acetylene was added to the system at a density of 1.2×10^{17} molecule cm^{-3}. Since an increase of a factor of two over the heterogeneous loss could have been observed with C_2H_2 present, an upper limit for the rate constant of the $C_4H_5 + C_2H_2$ reaction at 950K could be established. It is 2×10^{-14} cm^3 molecule^{-1} s^{-1}.

DISCUSSION

The simplest mechanism for the $C_4H_5 + O_2$ reaction which can account for the observations of this study and which is consistent with our current knowledge of the mechanisms of other unsaturated free radicals with molecular oxygen is one which involves the reversible addition of O_2 to the butadienyl radical and a second, irreversible decomposition path for the $C_4H_5O_2$ adduct.

Above 500K, C_4H_5 and O_2 establish and maintain equilibrium while the second, slower, irreversible decomposition reaction of $C_4H_5O_2$ takes place. These reaction pathways account for the observed high-temperature behavior of the $C_4H_5 + O_2$ reaction, including the exponential decay of C_4H_5 when O_2 is in excess, the proportionality of the C_4H_5 decay constants with $[O_2]$, and the lack of density dependence of the overall rate constant for the loss of C_4H_5. Under these conditions there is a relationship between the phenomenological rate constant k_4 and those of the elementary reactions responsible for the loss of C_4H_5, $k_4 = K_1 k_3^\infty/2$ (k_3^∞ is the high pressure limit unimolecular rate constant for reaction 3). Using the measured values of K_1 and k_4 an Arrhenius expression for k_3^∞ was determined, $k_3^\infty = 3 \times 10^{12} \exp(-21 \text{ kcal mol}^{-1}/RT) \text{ s}^{-1}$.

The rate constant derived for the decomposition of the adduct is very similar to that obtained for the decomposition of the $C_3H_3O_2$ adduct formed in the reaction of the propargyl radical with molecular oxygen.[3] Likewise, the R-O_2 bond strength when R is C_4H_5 is nearly identical with that when R is either C_3H_3 or C_3H_5 (see Table II). The mechanism proposed here for the $C_4H_5 + O_2$

reaction, i.e., reversible addition with a second, irreversible decomposition pathway for the RO_2 adduct, appears common to all R + O_2 reactions. The initial R-O_2 adducts are formed at rates expected for a simple combination process along an attractive potential. However, the R-O_2 bonds formed by the more stable unsaturated radicals are weaker (18 - 19 kcal mol^{-1}) than those formed between alkyl radicals and O_2 (32 - 38 kcal mol^{-1}). The overall reaction pathways observed and the nature of the final products are determined by the relative heights of the barriers to dissociation of the RO_2 adducts back to reactants and to rearrangement of the RO_2 adducts followed by dissociation into oxygenated products. If, as in the case of the allyl radical, the barrier to rearrangement is much greater than that to redissociation, no oxygenated products are observed and the R + O_2 reaction appears to "turn off" at high temperatures where the equilibrium favors the reactants. If, on the other hand, the barrier to rearrangement is only slightly higher than that to redissociation, the R/RO_2 equilibrium again favors reactants but small amounts of oxygenated products will be observed to be formed as the temperature increases. Such is the case in the C_3H_3 and C_4H_5 reactions. Finally, if the barrier to rearrangement is much less than to redissociation, the R + O_2 reaction appears to proceed directly to the oxygenated products as in the case of the i-C_4H_3 reaction.[4]

In conclusion, even at combustion temperatures, reactions of C_3H_3, C_3H_5, or C_4H_5 with molecular oxygen are not rapid. They do not effectively remove these intermediates from the pool of radicals. The loss mechanisms for these unsaturated radicals under combustion conditions must also include reactions with themselves to produce larger, unsaturated molecules, reactions with other free radicals (such as O and OH) and perhaps reactions with unsaturated molecules (such as acetylene or butadiene), reactions which could ultimately lead to the production of aromatic compounds.

ACKNOWLEDGEMENT

This research was supported by the Division of Chemical Sciences, Office of Basic Energy Sciences, Office of Energy Research, U.S. Department of Energy under grant No. DE/FG05-89ER14015.

REFERENCES

1. Westmoreland, P. R.; Dean, A. M.; Howard, J. B.; Longwell, J. P. *J. Phys. Chem.* **1989**, 93, 8171 and references therein.
2. Slagle, I. R.; Ratajczak, E.; Heaven, M. C.; Gutman, D.; Wagner, A. F. *J. Am. Chem. Soc.* **1985**, 107, 1838.
3. Slagle, I. R.; Gutman, D. *Twenty-First Symposium (International) on Combustion;* The Combustion Institute: Pittsburgh, PA, 1986; p 875.
4. Slagle, I. R.; Bernhardt, J. R.; Gutman, D. *Twenty-Second Symposium (International) on Combustion*; The Combustion Institute: Pittsburgh, PA, 1988; p 953.

Table I: Conditions and Results of the Study of the $C_4H_5 + O_2$ Reaction

a) Experiments to Measure $C_4H_5 + O_2$ Rate Constants

T[a], K	10^{-16}[M][b], molec. cm^{-3}	$10^{-11}[C_5H_8]_o$, molec. cm^{-3}	$10^{-10}[C_4H_5]_o$[c], molec. cm^{-3}	$10^{-14}[O_2]$ Range, molec. cm^{-3}	k_2, s^{-1}	$10^{14}k_1$[d], cm^3 $molec^{-1}$ s^{-1}
			Room Temperature Reaction			
296	6.00	7.11	3.20	1.93-13.4	37.8	23.
295	12.0	7.22	2.16	1.13-13.7	36.4	32.
299[e]	12.0	56.6	2.83	1.46-12.5	15.1	31.
296	18.0	2.69	2.64	1.10-9.52	35.9	38.
296	18.0	5.73	2.82	1.77-12.3	34.0	36.
299	18.0	1.27	1.16	1.22-9.34	31.5	38.
			High Temperature Reaction			
600[e]	6.02	7.82	3.46	60.7-216.	26.2	0.72
600[e]	12.0	28.5	11.0	17.7-172.	27.8	0.94
750[e]	6.02	50.1	8.94	29.7-188.	18.3	1.2
750[e]	12.0	20.0	9.00	60.7-215.	29.3	1.1
900[e]	6.07	18.0	7.65	12.8-256.	26.7	1.8
900[e]	12.1	6.55	11.1	54.7-237.	26.6	1.6

b) Experiments to Measure the Equilibrium Constant for the $C_4H_5 + O_2$ Reaction[f]

T[a], K	$10^{-11}[C_5H_8]_o$, molec. cm^{-3}	10^5P_{O2}, atm^{-1}	k_2, s^{-1}	R_{12}	m_1, s^{-1}	m_2, s^{-1}	$10^{-3}K_{eq}$[g], atm^{-1}
369	7.81	5.54	23.5	1.58	309.	34.0	32.2
369	7.82	9.37	19.0	2.70	318.	29.9	31.9
374	6.78	7.73	27.0	1.97	345.	33.2	27.0
374	6.78	6.62	22.4	1.47	333.	34.9	25.4
379	7.85	10.1	21.7	1.47	374.	38.9	17.2
379	11.7	23.7	23.1	3.86	674.	41.9	17.5
384	14.5	25.2	29.9	2.63	679.	45.0	11.1
384	15.4	44.3	28.4	4.37	833.	43.8	10.3
389	7.95	26.2	31.0	3.15	847.	54.7	13.0
389	14.9	26.2	31.4	2.64	702.	41.1	10.5
389	14.7	45.7	34.2	4.86	1193.	52.5	11.0
394[e]	107.	46.0	22.8	2.43	1215.	57.5	5.74
394	13.6	53.4	21.3	3.27	1071.	54.0	6.65
399	9.96	30.5	30.8	1.65	674.	53.4	6.06
399	9.84	56.6	26.3	2.26	892.	53.0	4.37

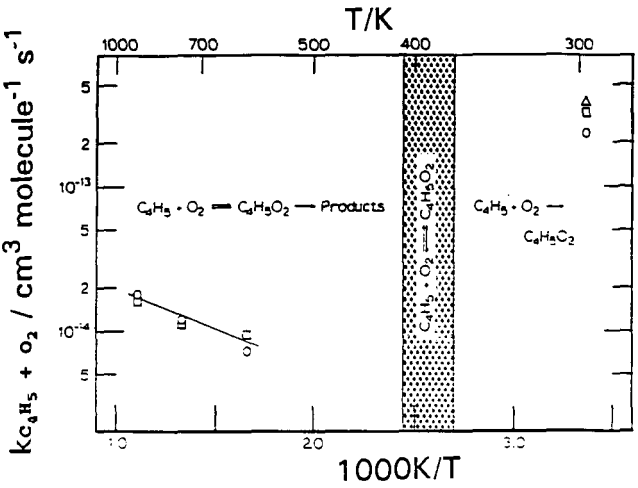

Figure 1. Arrhenius plot of measured second-order rate constants for the $C_4H_5 + O_2$ reaction. Shaded area indicates the temperature region where equilibrium was the dominant process observed. o indicates experiments conducted at a density of $6x10^{16}$, □ at $1.2x10^{17}$, and Δ at $1.8x10^{17}$ molecule cm^{-3}.

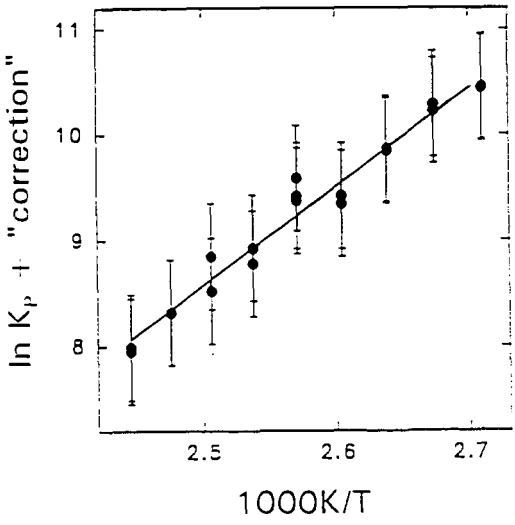

Figure 2. Modified van't Hoff plot of measured equilibrium constants for the $C_4H_5 + O_2$ reaction.

Table I (continued)

T[a], K	$10^{-11}[C_5H_8]_0$, molec. cm^{-3}	10^5P_{O2}, atm^{-1}	k_2, s^{-1}	R_{12}	m_1, s^{-1}	m_2, s^{-1}	$10^{-3}K_{eq}$[g], atm^{-1}
404	20.2	45.6	37.8	1.39	921.	76.3	3.54
409	20.2	46.2	29.4	0.809	580.	69.3	2.42
409	12.6	57.9	29.8	1.23	1001.	74.5	2.51

[a]Temperature variations: 350-450±3K, 600±2K, 750±4K, 900±5K
[b]M = He + O_2
[c]Upper limit to $[C_4H_5]_0$ estimated assuming that one half of the precursor that decomposes produces C_4H_5.
[d]Estimated error limits are ±20% for room-temperature rate constants and ±30% for high temperature rate constants.
[e]248 nm photolysis light used in this experiment; 193 nm used in all other experiments.
[f]C_4H_5 ion signal, I(t), fit to expression $I(t) = A\exp(-m_1t) + B\exp(-m_2t)$. [M] = 1.2×10^{17} molecule cm^{-3}
[g]$K_p = (R_{12}/P_{O2})\{1 + [(R_{12} + 1)(m_2 - k_w)][R_{12}(m_1 - m_2)]\}^2$; R_{12} = A/B; estimated error limits: ±50%.

Table II: Comparison of Thermodynamic Variables for R + O_2 Reactions Involving Unsaturated Free Radicals

R	ΔH°_{298}, kcal mol^{-1}	ΔS°_{298}, cal mol^{-1} K^{-1}	Ref.
C_3H_3	-18.9±1.4	-31.3±2.9	3
C_3H_5	-18.2±0.5	-29.2±1.2	2
C_4H_5	-18.7±0.8	-29.2±2.2	Current Study

The Thermal Decomposition of 1,7 Octadiyne as A Source of Propargyl Radicals

Wing Tsang and James A. Walker.
Chemical Kinetics and Thermodynamics Division
National Institute of Standards and Technology
Gaithersburg, Maryland 20899

Keywords: propargyl, shock tube, 1,7octadiyne

ABSTRACT

Dilute concentrations of 1,7 octadiyne have been decomposed in single pulse shock tube experiments. At temperatures between 1000-1200K and pressures of 2-7 atm argon, the products are consistent with the main reaction involving the breaking of the propargylic carbon-carbon. The rate expression for bond breaking is 1.6×10^{16} exp(-35760/T) s^{-1}. The newly formed pent-4-ynyl radical can cyclize or decompose via beta bond cleavage to form another propargyl radical and ethylene. The ratio of rate constants for the two processes is 5.4×10^{-4}exp(6700/T). A parallel retroene reaction proceeds with the rate expression, 5.6×10^{12}exp(-27860/T) s^{-1}. The propargyl radicals recombine to form a large number of linear C_6 isomers. As the temperature is increased fulvene and benzene are among the main products. The use of 1,7 octadiyne as a thermal source of propargyl radicals for studying reactions with other reactive species will be discussed.

INTRODUCTION

Recent studies[1,2] have demonstrated the important role that propargyl radicals may play as a precursor for the formation of benzene and other C_6H_6 isomers in hydrocarbon combustion systems. Except for the work on Kern and coworkers[3] at very high temperatures, there have been no direct quantitative studies involving the reactions of propargyl radicals with other organic molecules under conditions that lead to results that can be used in combustion systems. A prerequisite for making such studies is a method for the generation of propargyl radicals in known quantities. This paper reports on the results of efforts in this direction and on the nature of the products from propargyl radical combination.

Stein et al[1] have confirmed[4] that one of the possible products of propargyl radical combination, 1,5 hexadiyne will easily rearrange through molecular processes to form fulvene and benzene. Alkemade and Homann[2] have generated propargyl radicals through reaction of propargyl bromide with sodium and reported on the formation of a variety of recombination products, 1,5 hexadiyne, 1,3 hexadien-5-yne, 1,2 hexadien-5-yne, 1,2,4,5-hexatetraene and benzene at temperatures between 623-673K. They distinguish between initial and secondary products with benzene and 1,3-hexadien-5-yne being in the latter category. To some degree these results are discordant with that of Stein et al, since one would have thought that with the low energy molecular decomposition channel for 1,5 hexadiyne, most of this compound would have been immediately converted upon recombination in the low pressure system used by Alkemade and Homann. In addition, they were not able to detect the well known characteristic products of 1,5 hexadiyne decomposition, bis-methylenecyclobutene and fulvene.

The focus of this study is 1,7 octadiyne decomposition. Previously, extensive studies[5] on the decomposition of the larger acetylenes have been carried out. The important reaction pathways were the breaking of the propargyl C-C bond and a molecular process (retro-ene reaction) leading to the production of allene and the appropriate olefin. On this basis it is expected that the mechanism for 1,7 octadiyne decomposition will be

1,7 octadiyne -> propargyl + pent-4-ynyl	(1)
pent-4-ynyl -> propargyl + ethylene	(2)
pent-4-ynyl -> cyclopentenyl -> cyclopentadiene(C_5H_6)+H	(3)
1,7 octadiyne -> allene + pent-1-ene-4-yne (P1E4Y)	(4)

The desired reactions are (1) and (2) and it will be noted that every ethylene that is formed leads to the creation of two propargyl radicals. Reactions (3) and (4) are possible interfering processes. The consequence of (4) is not important since all that occurs is the release of two stable species into the system. Reaction (3) releases hydrogen atoms. This can lead to the formation of other radicals and to complications in the interpretation of the data. Such effects can be eliminated through the use of a chemical inhibitor. In addition, major contributions from this channel will mean that the 2 to 1 relation between propargyl and ethylene will be violated unless it is taken into consideration.

From another point of view the detection of cyclopentadiene is quite important since pent-4-ynyl is the result of the addition of propargyl to ethyene. Any products that are formed is indicative of ring closing becoming competitive with beta C-C bond cleavage leading to smaller molecular fragments. It is the competition between these two processes that is a key determinate of whether soot can be formed in any particular system.

In the course of this work experiments have also been carried out on the decomposition of 1,5 hexadiyne, 1-hexyne and 2,4 hexadiyne. All of these studies are aimed at providing confirmation for the surmise that a number of the gas chromatographic peaks that are observed arise from propargyl radical combination. This is necessary because it was not possible to identify specific compounds with these peaks.

Experiments are carried out in a single pulse shock tube. Such studies have unique capabilities for determining the stability characteristics (in the sense of unimolecular decompositions) of volatile organics at high temperatures. We have used the method for studying the thermal unimolecular decomposition processes of many organic compounds[6]. More recently, the mechanisms and rate constants for hydrogen-atom attack on unsaturated compounds[7] have been determined. For these studies, the hydrogen atoms were generated through the thermal decomposition of organic molecules in a manner similar to the generation of propargyl radicals in this study.

EXPERIMENTAL

The details of the single pulse shock tube and the experimental procedure[6] used in carrying out experiments on the thermal decomposition of organics have been described in earlier publications. Summarizing briefly, trace quantities of the organic in question, 100-1000 ppm, are decomposed by the reflected shock in the presence of large amounts of a thermally stable

chemical inhibitor such as mesitylene. Reactive radicals such as hydrogen atoms will attack the inhibitor leading to the formation of a less reactive, resonance stabilized species, 3,5 dimethylbenzyl radical. In the short time scale of shock tube experiments these can only recombine with itself and other long lived radicals and therefore can not play a role in the overall reaction. Analysis was by gas chromatography using flame ionization detection. The light gases were eluted isothermally using a 12 ft Poropak N^8 column while the heavier compounds, from C_4 on up, were eluted using a wide bore 30-meter dimethylsiloxane column in the programmed temperature mode. All products were identified on the basis of retention times of neat samples.

The experiments were carried out using the internal standard method. This eliminated the possibility of errors arising from uncertainties in the reaction temperature. The internal standard used in these experiments was the decomposition of 4-methylcyclohexene to form propene and butadiene. The rate expression for this reverse Diels-Alder reaction has previously been found to be

$$k(\text{4-methylcyclohexene}\rightarrow\text{propene+butadiene})=2\times10^{15}\exp(-33400/T)\,s^{-1}$$

The use of the inhibitor makes impossible chain processes. Thus the only decomposition process must be the initial unimolecular reactions. It is expected that resonance stabilized radicals such as propargyl should not be particularly reactive with trimethylbenzene in the time scale of the experiments. Of course it can react with the benzylic type radicals that are generated in the course of the inhibition reactions. These are chain terminating processes.

DISCUSSION

The important products bearing on decomposition mechanisms for dilute quantities of 1,7 octadiyne in mesitylene and argon are listed in Table 1. It is clear that the dominating channels are the breaking of the propargylic C-H bond and the retroene reaction leading to the formation of allene and pent-1-ene-4-yne (P1E4Y). It can be seen that the concentration of the specific products formed; ethylene, cyclopentadiene, and P1E4Y is very close to the amount of the 1,7 octadiyne that is destroyed. Significant quantities of allene and propyne were also found. A large portion of the former is due to the retroene reaction. The excess quantities may be formed through a variety of other mechanisms. Note that as discussed subsequently, under certain conditions substantial quantities of propargyl radicals actually survive the heating period and it is possible that propargyl radical may undergo a variety of other unspecified reactions. Small quantities of meta-xylene was also found. This is evidence that hydrogen atoms are present in the system. Since the branching ratio for hydrogen atom attack on mesitylene have been determined, the total number of hydrogen atom released into the system can be placed on a quantitative basis. The concentrations found here are somewhat larger than that which can be accounted for by cyclopentadiene formation. However, any hydrogen atom in the system will in fact reveal its presence through the presence of meta-xylene.

In the time range where one expects C_6H_6 compounds to elute under the

present conditions a large number of peaks were detected. Unfortunately, it was not possible to obtain the neat samples that would lead directly to the identification of many of these compounds. Typical chromatograms in this elution region can be found in Figure 1. At low conversions (and temperatures) one sees the initial formation of a plethora of products. At high conversions and temperatures one notes increasingly the formation of fulvene and benzene as well as smaller quantities of other unidentified products.

An important question is whether these peaks can actually be attributed to the combination of propargyl radicals. The results of ancillary experiments with 1,5 hexadiyne, 1-hexyne and 2,4 hexadiyne are as follows. In the case of 1-hexyne, where the mechanism involve formation of the propargyl radical, many of the same peaks that were found in the decomposition of 1,7 octadiyne were also present. Unfortunately the parent hexyne-1 pick eluted at the same time as the fulvene peak. In the case of 1,5 hexadiyne the situation is similar to that found by Stein and coworkers, dimethylenecylobutene is first formed, followed by conversion into fulvene and benzene. Typical chromatograms can be found in Figure 2. It is interesting to note that in the studies with 1,7 octadiyne and 1-hexyne, 1,5 hexadiyne could barely be detected. Nevertheless the pattern of products, in these studies were very much similar to that found in the direct 1,5 hexadiyne decomposition. The obvious interepretation is that 1,5 hexadiyne is an important intermediate. The existence for this molecule of very low energy decomposition channels mean that at the high temperatures of these studies they are almost immediately converted into the stable decomposition products, fulvene and benzene. 2,4 Hexdiyne is a minor product. Its decomposition product was found to be chiefly benzene and a small quantity of fulvene. These results clearly establish that from the linear C_6H_6 isomers there must be a variety of pathways to form benzene. In the present instance benzene must be formed after various hydrogen shifts.

Quantitative results can give a better picture of the rate at which propargyl radicals are generated in this system. The analysis of this data and the determination of the appropriate rate constants and expressions follow from earlier publications. In the present case the propargyl C-C bond cleavage is monitored by the yield of ethylene and cyclopentadiene. The contribution from the molecular retro-ene reaction is determined from the yields of the pent-1-ene-4-yne (P1E4Y). The rate constants can be related to the measured yields on the basis of the following relations

$$k(1) = \log(1-X*C_2H_4+\text{cyclopentadiene}/(1,7\text{cyclooctadiyne})_i)/X*t$$
$$k(4) = k(1)*(\text{P1E4Y})/C_2H_4+\text{cyclopentadiene}$$

where X = 1 + (P1E4Y)/C_2H_4+cyclopentadiene, t is the total heating time of approximately 500 microsec. A plot of these results can be found in Figure 1. The rate expressions for the two initial processes are therefore

$$k(1)=1.6\times10^{16}\exp(-35760/T)\ s^{-1}$$
and
$$k(4)=5.6\times10^{12}\exp(-27860/T)\ s^{-1}$$

It should be noted that the reaction temperature is calculated on the basis of the propene yields from 4-methylcyclohexene decomposition and is derived from the relation 1/T = (log k(4-methylcyclohexene=propene+1,3butadiene)-

LogA)/E, where the A and E are rate parameters for 4-methylcyclohexene decomposition decomposition given earlier.

It is interesting to compare these rate expressions with that for 1-hexyne decomposition. The rate expressions are

$$k(\text{hexyne-1=propargy + n-propyl})=8\times10^{15}\exp(-36300/T)s^{-1} \text{ and}$$
$$k(\text{hexyne-1=allene+}C_3H_6)=5\times10^{12}\exp(-28400/T)s^{-1}.$$

At the reaction temperature the differences in rate constants are factors of 3.3 and 1.8 respectively. For the latter this is very close to the reaction pathway degeneracy. On the other hand for the bond breaking process the rate constant for 1,7 octadiyne decomposition is a factor of 1.7 higher than would be dictated by the two propargyl bond. From the rate expressions, it would appear that this is an activation energy effect, although this claim cannot be completely justified in terms of the uncertainties in deriving the rate expression. It appears that propargyl substitution in the beta position has a larger than expected effect on rate constants for bond cleavage. Studying octyne-1 decomposition will be very worthwhile.

The ratio of cyclopentadiene to ethylene yields a measure of the branching ratio for pent-4-ynyl decomposition. An Arrhenius plot of this ratio can be found in Figure 2. The rate expression is

$$k(3)/k(2)=5.4\times10^{-4}\exp(6700/T)$$

In the temperature range of these experiments this is equivalent to 25% cyclization at the lowest temperatures and decreasing to 10% at the other extreme. Cyclization is thus favored at the lower temperatures and the activation energy for cyclization is about 50 kJ/mol smaller than that for beta C-C bond fission. This is a surprisingly large number since with an estimated activation energy for C-C bond fission of about 120 kJ/mol will lead to an activation energy for cyclization in the 80 kJ/mol range. It is also possible that this process is not kinetically controlled and that the ratio given above is a reflection of the equilibrium properties of the cyclic and linear radicals. Obviously further work is required. For the present purposes it is clear that optimum yields of propargyl radicals will be acheived at the highest temperatures. At 900 K cyclization and beta bond cleavage will be equally important.

With this data there is now sufficient information to deduce the temporal history of propargyl in the present system. Using a rate expression for propargyl combination similar to that for allyl[9], it was found that at lower concentrations, 200 ppm level and 2 atms pressure, a large portion of the radical remain unreacted during the entire heating period and much of the products are thus presumably formed at somewhat lower temperatures. On the other hand for the higher concentrations 1000 ppm and 7 atms. recombination is substantially completed in during the heating period. Despite this difference the chromatograms are substantially similar. In addition, recovery in the form of the C_6H_6 compounds is no more than 50% of all the propargyls that are released into the system. Here again the results appear to be independent of the concentration of radicals released into the system. The former may be a reflection of the low energy pathways available for decomposition and the formation of hot molecules from

propargyl recombination. Propargyl radicals can of course also be removed from the system by combination with 3,5 dimethylbenzyl and methyl radicals. These pathways cannot account for all the deficit.

The results are in general confirmatory of the observations of Stein et al regarding the nature of the decomposition products of 1,5 hexadiyne decomposition and that of Homann and Alkemade regarding the wide variety of linear C_6H_6 compounds that can be formed. Indeed the present results suggest many more peaks than the latter reported. It is difficult to account for the failure of Alkemade and Homann to find two of the decomposition products of 1,5 hexadiyne pyrolysis, dimethylenecyclobutene and fulvene. This is particularly serious for fulvene since it apparently is quite stable as the temperature is increased. It is possible from the reported retention times of Alkemade and Homann the 1,3 hexadiyne-5 and fulvene peaks may actually be coincident.

A system for the controlled release of propargyl radicals have now been described. The next step in this work must be studies where the propargyl radicals are allowed to react with other unsaturated compounds or radicals that may be present in high temperature reactive systems. A major problem in so far as single pulse shock tube studies are concerned is that the reaction time is very short and if truely quantitative results are to be obtained concentration of propargyl or reactants must be maintained at a sufficiently high level so that all the reactions occur during the heating period. With such a scenario, measurements of the concentration of one of the direct propargyl combination products, for example, benzene, and the product of addition or combination with another species can now be used as a means of determining relative rate constants. This can lead to a scale of propargyl reactivities and predictions regarding the quantity and distribution of the aromatic products formed in high temperature pyrolytic systems. Comparison with actual measurements will then lead to an assessment of the actual importance of propargyl radical in soot forming systems.

REFERENCES

1. Stein, S. E., Walker, J. A., Suryan, M. M. and Fahr, A. 23rd Symposium on Combustion, in press

2. Alkemade, U, and Homann, K. H., Zeit. Phys. Chemie Neue Folge. Bd 161, 19, 1989

3. Wu, C. H. and Kern, R. D., J. Phys. Chem., 91, 6291, 1987

4. Brown, R. F. C., "Pyrolytic Methods in Organic Chemistry",Academic Press, 1980 pg. 324

5. Tsang, W. Int. J. Chem. Kin., 10, 687, 1978

6. Tsang, W.,"Comparative Rate Single Pulse Shock Tube in the Thermal Stability of Polyatomic Molecules," Shock Tubes in Chemistry, A. Lifshitz ed., Marcel Dekker, pg. 59, 1981.

7. Cui, J. P., He, Y. Z., and Tsang, W., J. Phys. Chem, 93,724, 1989

8. Certain commercial materials and equipment are identified in this paper in order to specify adequately the experimental procedure. In no case does such identification imply recommendation of endorsement by the National Institute of Standards and Technology, nor does it imply that the material or equipment is necessarily the best available for the purpose.

9. Tulloch, J. M., MacPherson, M. T., Morgan, C. A., and Pilling, M. J., J. Phys. Chem.,86, 3812, 1982

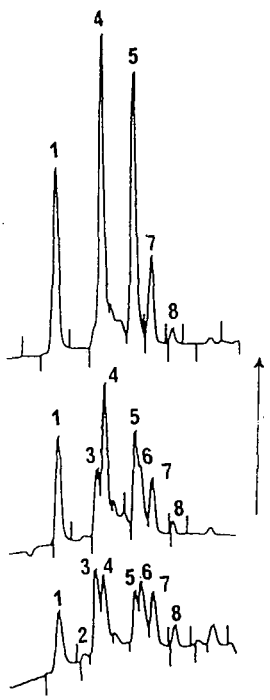

Figure 1. Typical chromatograms in the C_6 region from 1,7 Octadiyne decomposition. Peaks 1,6-8 were not identified. (2)=1,5hexdiyne (3)= dimethylenecyclobutene (4)=fulvene (5)=benzene. Arrow points to higher temperature.

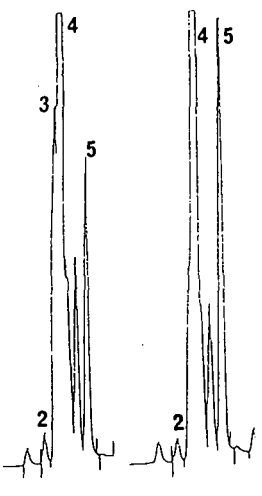

Figure 2. Typical chromatograms in the C_6 region from 1,5 hexadiyne decomposition (2)=1,5hexadiyne, (3)= dimethylenecyclobutene (4)= fulvene, (5)=benzene. Arrow points to higher temperature.

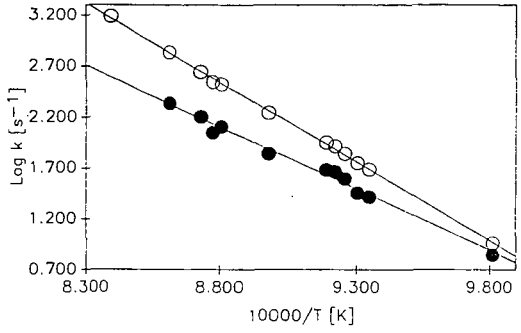

Figure 3. Arrhenius plots for the decomposition of 1,7 octadiyne. (○) propargyl C-C bond cleavage. (●) retroene reaction

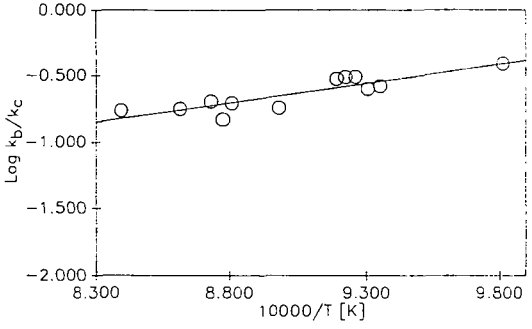

Figure 4. Arrhenius plot for the ratio of rate constants for cyclization vs beta bond cleavage during the decomposition of pent-4-ynyl

Table 1. Reactant and Product Distribution formed from 1,7 Octadiyne Decomposition in the Presence of Excesses of Mesitylene

Temp.	Pressure (atm)	C_2H_4	Allene	Compounds (%conversion) Propyne	P1E4Y	C_5H_6	1,7oct
a. 200 ppm 1,7 octadiyne in 0.5% Mesitylene and Argon							
1080	1.8	1.1	.9		.7	.2	100
1101	2.1	6.1	4.3	.6	4.1	1.5	87
1131	1.8	13.7	8.2	1.3	6.7	2.5	72
1150	1.9	21.9	11.1		10.1	4.9	52
1166	2.2	31.0	15.4	4.7	10.8	5.5	44
b. 1000 ppm 1,7 octadiyne and 1.0% Mesitylene and Argon							
1034	1.8	.8	.8	.1	.8	.3	92
1101	2.1	6.1	4.3	.6	3.9	1.3	75
1141	6.2	17.7	10.5	3.0	8.8	3.7	65
1183	6.7	43.1	19.3	7.4	11.8	7.4	27

THE REACTIONS OF PROPARGYL CHLORIDE AND 1,5 HEXADIYNE BEHIND REFLECTED SHOCK WAVES

R.D. Kern, K. Xie and H. Chen
Department of Chemistry
University of New Orleans
New Orleans, Louisiana 70148

Keywords: propargyl radicals, benzene formation, shock waves

INTRODUCTION

Several reports have appeared which describe the reactions of C_3H_3 and the subsequent formation of benzene. These investigations have been conducted using a variety of experimental techniques and precursor compounds to form propargyl radicals: allene,[1] 1,2 butadiene[2] (shock tube); 1,5 hexadiyne[3] (flow reactors); ethylacetylene[4] (microjet reactor); rich acetylene flames;[5,6] C_3H_3Cl or C_3H_3Br + Na[7] (flow reactor); allene and propyne[8] (shock tubes). Although there is general agreement that the reaction of 2 C_3H_3 ---> C_6H_6 is an efficient route to benzene, there are several C_6H_6 isomers such as bisallene, 3,4 dimethylenecyclobutene, and fulvene that have been proposed to participate in the sequence of reactions that precede benzene formation[9] and consensus is lacking on the details of the conversion.

Furthermore, reactions of C_3H_3 with allene and propyne have been proposed[1] as routes to benzene via the sequence $C_3H_3 + C_3H_4$ ---> C_6H_7 ---> C_6H_6 + H. The single pulse shock tube results of Hidaka et al. indicate that benzene yields are greater in the pyrolysis of allene compared to those recorded from a mixture containing an equivalent amount of propyne.[8]

There has been considerable effort expended on the allene ⇌ propyne isomerization by experimentalists and theoreticians which is described in a recent review.[10] The energetics of various intermediates involved in the isomerization such as trans-vinylmethylene, cyclopropene, and propenylidene have been calculated and the highest energy barrier, 65.8 kcal/mol, identified.[11]

The object of this work is to examine the reactions of two possible precursors for C_3H_3, propargyl chloride and 1,5 hexadiyne, and to study the reactions of C_3H_3 with itself and with allene (C_3H_4A) and propyne (C_3H_4P) with particular emphasis on the formation of benzene. This latter point is important since a correlation between benzene production and soot yield has been proposed.[12]

EXPERIMENTAL

A shock tube coupled to a time-of-flight (TOF) mass spectrometer is employed to analyze dynamically the reflected shock zone containing various mixtures of gases. The apparatus and experimental procedures have been described recently.[10] The mixture compositions and reaction conditions are listed in Table 1.

The sources of reactants are as follows: C_3H_3Cl (Aldrich, 98%); C_3H_4A (Matheson, 93%); C_3H_4P (Farchan); 1,5 C_6H_6 (Alpha); D_2 (Matheson, 99.5%); H_2 (Linde, 98.5%); Ne (Matheson, 99.999%). Ionization was achieved by 32 eV electron bombardment. The mass spectral range covers m/e 12 - 120. Peak heights were converted to concentrations using calibration plots obtained under no-reaction temperatures. The following mixtures diluted with neon were prepared for the calibration of the corresponding species: 3% C_3H_3Cl; 3% C_3H_4A; 3% C_3H_4P; 2% 1,5 C_6H_6; 3.2% C_2H_2; 2% HCl; 2% C_4H_2; 2% C_6H_6; and 3% CH_4. The mass spectral factor for C_6H_2 was obtained from previous work in which a carbon atom balance procedure was employed.[13]

RESULTS AND DISCUSSION

Mixtures A, B, and C: 3% C_3H_3Cl decomposes readily at temperatures above 1400 K. Major products are C_2H_2, HCl, and C_4H_2 which were observed to form at the same reaction time. The amount of HCl formed is equal to the amount of dissociation of propargyl chloride, indicating that Cl atom is balanced. However, carbon atom balance is only 60 - 80%. Concentration plots for 3% C_3H_3Cl pyrolysis at 1411 K are shown in Figures 1 - 4. Solid lines represent model calculations using the mechanism listed in Table 2. The C_3H_3Cl mass spectral cracking pattern displays a substantial peak at m/e 39 ($C_3H_3^+$). At late reaction times, m/e 39 disappears but m/e 74 remains, indicating the formation of C_6H_2.

Benzene was not recorded in the thermal decomposition of 3% C_3H_3Cl. However, upon addition of 5% H_2 (mixture B), benzene was detected. The major products distribution and the carbon balance are the same as in the decomposition of 3% C_3H_3Cl; Cl atoms are balanced. The results from 3%C_3H_3Cl - 5% D_2 (mixture D) are interesting. HCl and DCl are formed almost at the same time; the temporal HCL/DCl ratio is ~ 5. The following two parallel initation reactions are proposed to account for the experimental results:

$$C_3H_3Cl \quad \text{---}> \quad C_3H_3 + Cl \quad (17\%) \qquad (1)$$

$$\text{---}> \quad C_3H_2 + HCl \quad (83\%) \qquad (2)$$

Mixtures D and E: Compared to the pyrolysis of 3% C_3H_3Cl, 1,5 hexadiyne decomposes at relatively higher temperatures. The major products are C_2H_2, C_4H_2, and C_6H_2. Carbon balance for 2% 1,5 C_6H_6 pyrolysis is 75 - 80% in the temperature range 1657 - 1800 K. Adding 5% H_2 does not change the product distribution but results in 100% carbon balance due to the increased amount of observable products. Benzene production was difficult to determine here due to the overlap of the parent molecule and benzene.

Mixtures F and G: The TOF results for a 4.3% allene mixture are published in ref. 1. We employed 3% allene or propyne mixtures here in order to maintain the same carbon atom concentrations as most other mixtures in Table 1 and to compare the respective benzene yields. 3% allene and 3% propyne mixtures were shocked at the same experimental conditions to determine if there are any kinetic differences as claimed in the single pulse shock tube work.[8] Benzene is formed in amounts of 2.3 - 3.2 x 10^{-9} mol/cm^3, about the same levels as in mixtures H and I. CH_4 is a minor product. The carbon atom balance is ~90%. The reaction profiles were modeled by the mechanism of ref. 1. Figures 5 - 8 show 3% propyne decomposition at 1770 K. Examining the C_3H_4 and the product concentrations, it is concluded that there are little or no observable differences between these two isomers at high temperatures which confirms that the isomerization reaction is faster than the decomposition.

Mixtures H and I: There are no significant differences in comparing the reaction profiles for these two mixtures. Benzene appears in amounts of 2.5 x 10^{-9} to 4.0 x 10^{-9} mol/cm^{-3} for the temperature range 1325 - 1735 K. Major products are C_2H_2, C_4H_2, HCl. Comparison of the respective profiles reveals that propargyl chloride decomposes much faster than allene or propyne. The C_3H_3Cl profile is obtained by Cl atom balancing, since its mass spectral sensitivity is low and interference from C_6H_2 at high temperatures is severe. The reaction profiles for mixtures H and I at 1458 and 1492 K are displayed in Figures 9 - 16.

The mechanism in Table 2 is composed of the previous allene mechanism[1] and reactions of propargyl chloride. Benzene appears at lower temperatures in H and I compared to F and G and is formed mainly from the overall net reaction

$$C_3H_2 + C_3H_4 \text{ ----> } [2\ C_3H_3] \text{ ----> } C_6H_6$$

Benzene production predicted by the model is about 4 times higher than the experimental data as shown in Figures 12 and 16. The carbon atom balance for the two mixtures are about 70% at ~ 1450 K. This carbon deficiency is due to the formation of high molecular weight polyaromatic

hydrocarbons (PAH) and solid carbon; these steps are not included in our mechanism. The model describes reasonably well the observable species except for benzene. The overall reactions (3) and (4) are highly exothermic. It is likely that benzene or its isomers, some of which are highly reactive, are apparently consumed in a series of reactions leading to PAH and soot. The mechanism is tentative; extensive modeling of the experimental data is ongoing.

Mixtures J and K: C_2H_2, C_4H_2, and C_6H_2 are the detectable products. Reaction profiles and product distributions are the same as for mixtures J and K at similar reaction conditions. Carbon balance is around 70%. Information relevant to benzene formation is obscured due to the overlap of the parent peak.

CONCLUSIONS

The main decomposition channel for propargyl chloride pyrolysis is through the elimination of HCl to form C_3H_2. C_3H_2 plays an important role in producing benzene in reactions with allene or propyne. Benzene is not observed in the pyrolysis of C_3H_3Cl but it is formed readily in mixtures of C_3H_3Cl and allene or propyne.

ACKNOWLEDGEMENTS: The research is supported by the U.S. Department of Energy under contract DE-FG0585ER/13400.

References

1. Wu, C.H. and Kern, R.D., J. Phys. Chem., 91, (1987), 6291.
2. Kern, R.D., Singh, H.J. and Wu, C.H., Int. J. Chem. Kinet., 20, (1988), 731.
3. Stein, S.E., Walker, J.A., Suryan, M.M. and Fahr, A., 23rd Symp. (Int.) on Combustion, 1990, in press.
4. Boyle, J. and Pfefferle, L., J. Phys. Chem., 94, (1990), 3336.
5. Miller, J.A. and Melius, C.F., private communication.
6. Communal, F., Thomas, S.D. and Westmoreland, P.R., 23rd Symp. (Int.) on Combustion, 1990, poster paper P40.
7. Alkemade, V. and Homann, K.H., Z. Phys. Chem., 161, (1989), 19.
8. Hidaka, Y., Nakamura, T., Miyauchi, A., Shiraishi, T. and Kawano, H., Int. J. Chem. Kinet., 21, (1989), 643.
9. Brown, R.F.C., Pyrolytic Methods in Organic Chemistry, Vol. 41, p. 324, Academic Press, New York (1980).
10. Kern, R.D. and Xie, K., Prog. Energy Combust. Sci., 17, (1991), 191.

11. Yoshimine, M., Pacansky, J. and Honjou, N., J. Am. Chem. Soc., 111, (1989), 4198.
12. Kern, R.D., Wu, C.H., Yong, J.N., Pamidimukkala, K.M. and Singh, H.J., Energy & Fuels, 2, (1988), 454.
13. Wu, C.H., Singh, H.J. and Kern, R.D., Int. J. Chem. Kinet. 19, (1987), 975.

Table 1: Summary of Experimental Conditions

Mixture	Composition	T_5, K	P_5, atm
A	3% C_3H_3Cl	1411 - 1608	0.24 - 0.29
B	3% C_3H_3Cl - 5% H_2	1394 - 1633	0.24 - 0.31
C	3% C_3H_3Cl - 5% D_2	1364 - 1616	0.23 - 0.31
D	2% 1,5 C_6H_6	1530 - 1800	0.28 - 0.37
E	2% 1,5 C_6H_6 - 5% H_2	1367 - 1827	0.24 - 0.39
F	3% C_3H_4A	1564 - 2136	0.27 - 0.45
G	3% C_3H_4P	1549 - 2131	0.27 - 0.44
H	1.5% C_3H_3Cl - 1.5% C_3H_4A	1295 - 1698	0.20 - 0.32
I	1.5% C_3H_3Cl - 1.5% C_3H_4P	1304 - 1793	0.20 - 0.35
J	1.5% 1,5 C_6H_6 - 1.5% C_3H_4A	1316 - 1931	0.22 - 0.43
K	1.5% 1,5 C_6H_6 - 1.5% C_3H_4P	1438 - 1823	0.26 - 0.39

Table 2. Reaction Mechanism

	Reactions	A	E
1.	$C_3H_3Cl = C_3H_3 + Cl$	1.0E13	65.5
2.	$C_3H_3Cl = C_3H_2 + HCl$	5.0E13	65.5
3.	$C_3H_2 + C_3H_4A = C_6H_6$	4.0E11	0.0
4.	$C_3H_2 + C_3H_4P = C_6H_6$	4.0E11	0.0
5.	$C_3H_2 + C_3H_4A = 3\ C_2H_2$	1.7E13	15.0
6.	$C_3H_2 + C_3H_4P = 3\ C_2H_2$	1.7E13	15.0
7.	$2\ C_3H_2 = C_2H_2 + C_4H_2$	2.0E13	8.5
8.	$2\ C_3H_2 = C_6H_2 + H_2$	2.0E13	8.5
9.	$Cl + H_2 = HCl + H$	8.3E13	5.5
10.	$C_3H_4A = C_3H_4P$	2.0E13	62.0
11.	$C_3H_4A + M = C_3H_3 + H + M$	1.0E17	70.0
12.	$C_3H_4P + M = C_3H_3 + H + M$	1.0E17	70.0
13.	$C_3H_4A + H = C_2H_2 + CH_3$	2.0E13	2.4
14.	$C_3H_4P + H = C_2H_2 + CH_3$	2.0E13	2.4
15.	$C_3H_4P = C_2H + CH_3$	4.2E16	100
16.	$C_3H_4P + H = C_3H_3 + H_2$	1.0E12	1.5
17.	$C_3H_4A + H = C_3H_3 + H_2$	1.0E12	1.5
18.	$C_3H_4P + C_2H = C_3H_3 + C_2H_2$	1.0E13	0.0
19.	$C_3H_4A + C_2H = C_3H_3 + C_2H_2$	1.0E13	0.0
20.	$C_3H_4P + CH_3 = C_3H_3 + CH_4$	2.0E12	7.7
21.	$C_3H_4A + CH_3 = C_3H_3 + CH_4$	2.0E12	7.7
22.	$C_3H_3 + CH_3 = C_2H_5 + C_2H$	1.0E13	37.5
23.	$2\ CH_3 = C_2H_6$	2.0E13	0.0
24.	$C_3H_3 + CH_3 = C_4H_6$	5.0E12	0.0
25.	$C_3H_4A + C_3H_3 = C_6H_6 + H$	2.2E11	2.0
26.	$2\ C_3H_3 = C_6H_6(L)$	6.0E13	0.0
27.	$2\ C_3H_3 = C_6H_6$	3.0E11	0.0
28.	$2\ C_3H_3 = 3\ C_2H_2$	5.0E11	0.0

Units are: cm^3, mol, sec, kcal. Reactions 10 - 28 taken from ref. 1.

FIGURE 1

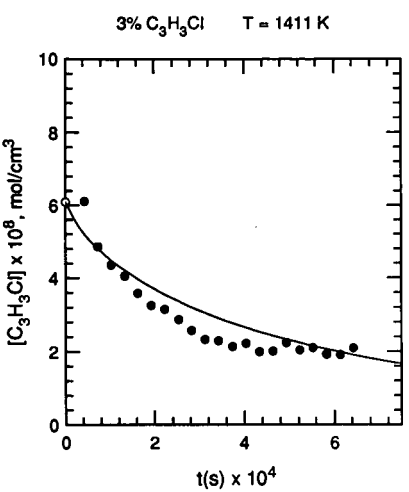

FIGURE 2

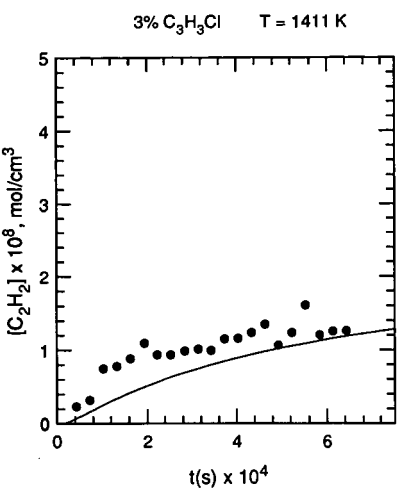

FIGURE 3

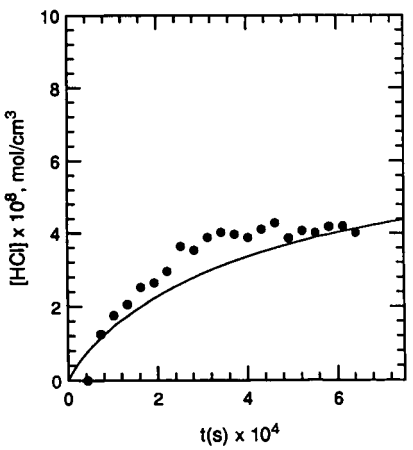

FIGURE 4

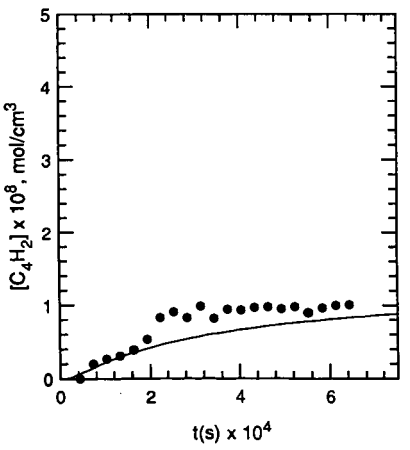

FIGURE 5

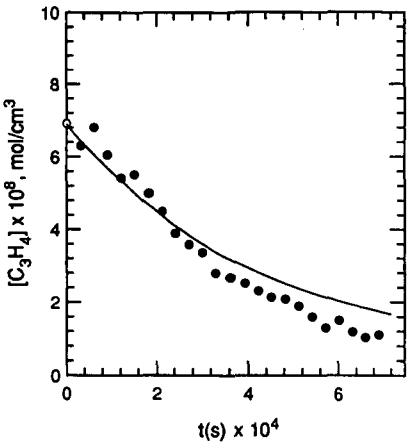

FIGURE 6

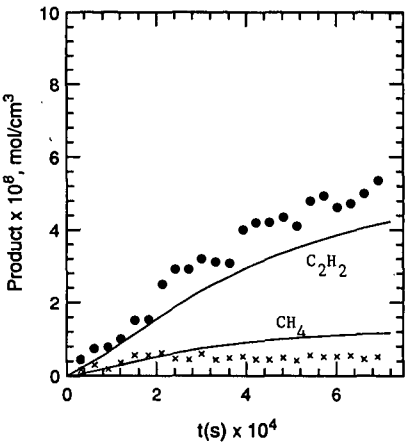

FIGURE 7

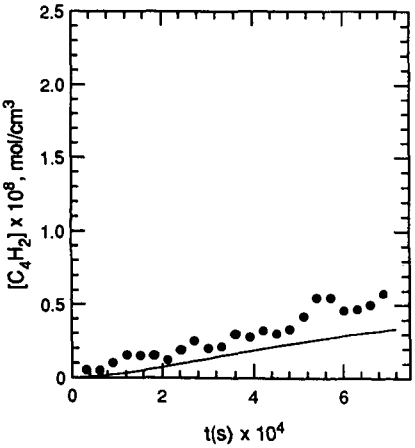

FIGURE 8

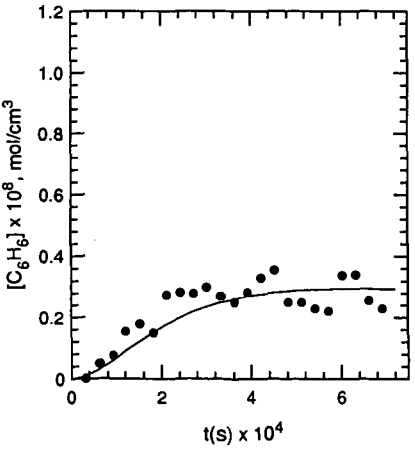

FIGURE 9

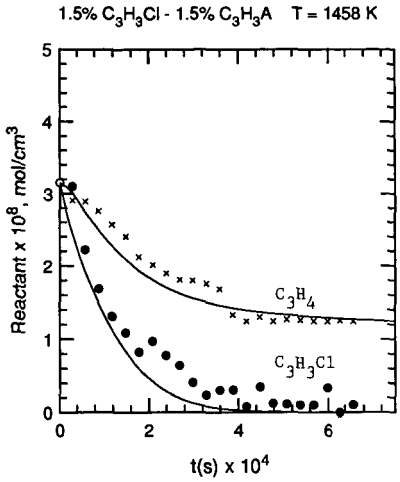

FIGURE 10

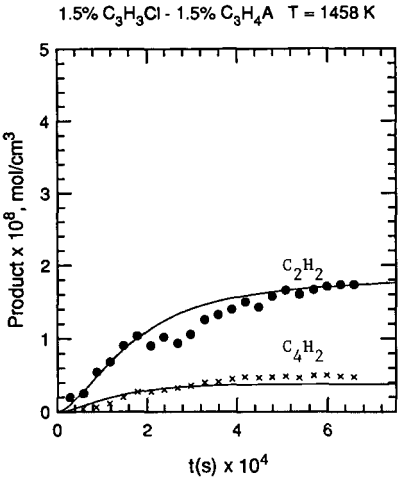

FIGURE 11

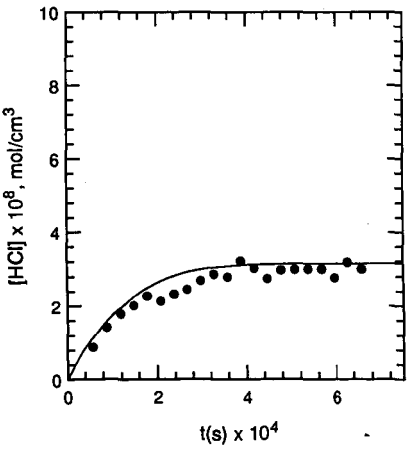

FIGURE 12

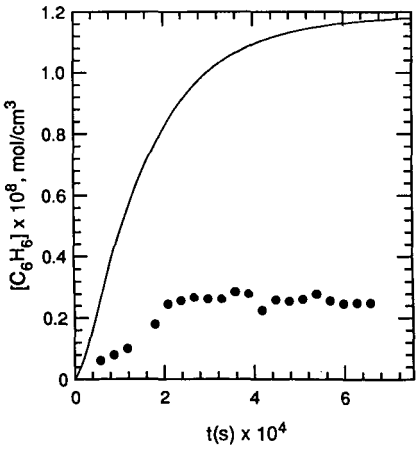

FIGURE 13

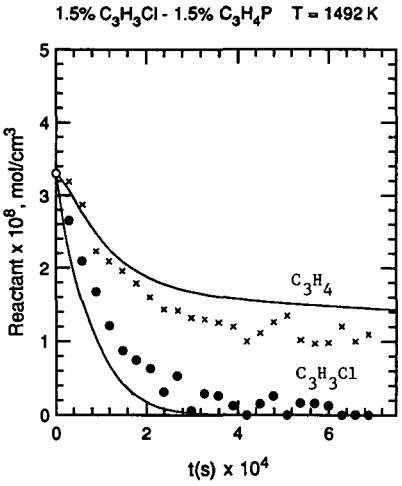

FIGURE 14

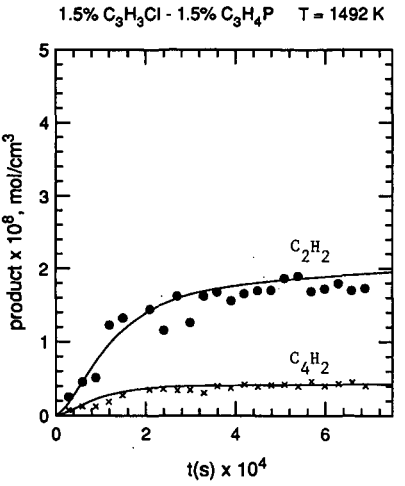

FIGURE 15

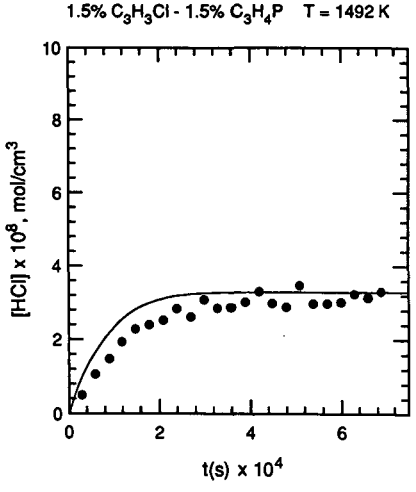

FIGURE 16

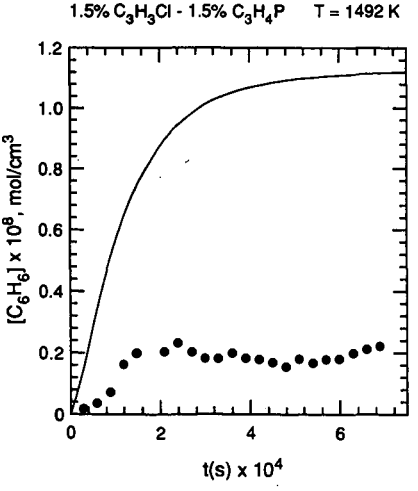

Benzene Formation during Allene Pyrolysis: Possible Implications for Soot Formation

L. D. Pfefferle, J. Boyle, and G. Bermudez
Department of Chemical Engineering, Yale University
New Haven, CT 06520-2159YS

Introduction

Pyrolysis of allene in a microjet reactor at millisecond reaction times was used to study higher hydrocarbon growth processes from C3 hydrocarbon species. Species detection was carried out using VUV photoionization mass spectrometry. The first product observed as temperature was increased at a fixed mean residence time was mass 80 followed by smaller than parent mass pyrolysis products, mass 79 and a possible allene trimer at mass 120. A mechanism for higher hydrocarbon formation in the pyrolysis of allene is proposed . Allene dimerization to a dimethylenecyclobutane is proposed as the initial higher hydrocarbon production mechanism during allene pyrolysis and this route is examined for thermodynamic plausibility.

Background

It has become increasingly apparent in the past several years that C_3 routes for soot formation in flames can be important under some if not many conditions. In several recent studies of fuel pyrolysis and combustion where both stable and labile product measurements were made (1a,b,2), C_4/C_2 routes for benzene production were determined to be not fast enough to account for observed benzene production for some of the fuels used, especially those of C_2 and C_3 hydrocarbons. Westmoreland (1b) has recently made a reaction pathway study of C_3H_3 dimerization to benzene using a QRRK analysis and concluded that this route could in fact be fast enough to account for observed benzene production rates in several test flames including acetylene and ethylene.

Allene dimerization to dimethylenecyclobutane isomers has been observed at high conversion in several early flow reactor pyrolysis studies (e. g. 3,4). In one study (3), primarily the 1,2-dimetheyenecyclobutane isomer (1,2 DMCB) was produced at about 50% yield by passing allene over quartz chips at 800K with a 6s mean residence time. The reactor geometry used, however, did not preclude the possibility of significant surface effects on the rate of dimethylenecyclobutane production and a run with an empty tube reactor gave somewhat lower conversion but the same product distribution. In the current study, mass 80 was the first product detected and the detection of mass 120 (a possible allene trimer) at slightly higher temperatures is consistent with allene dimerization to dimethylenecyclobutane as the initial pathway for higher hydrocarbon formation. Although the DMCB isomers are likely the first mass 80 species formed, at higher temperatures (over 1300K) the predominant mass 80 component is likely hexadienes. The reaction pathways for formation of the various mass 80 isomers is the focus of our continuing modeling work. This study investigates the

feasibility of the DMCB production through allene dimerization and how it can contribute to early higher hydrocarbon production during allene pyrolysis. It should be noted that from our previous work (2) methyl acetylene pyrolysis when carried out at temperatures and reaction times where isomerization to allene was not significant did not result in either significant mass 80 production or benzene production. This is consistent with mass 80 formation through allene dimerization.

Experimental Procedure

Allene pyrolysis was carried out in a microjet reactor source, described in detail earlier (5). This is a miniature fast-flow reactor coupled directly to a sonic nozzle with a volume of approximately 3.2×10^{-9} m^3. The reactor geometry consists of an alumina multibore thermocouple insulator tube inserted into a larger alumina tube with a sapphire nozzle (50-200 mm). The inner tube is positioned to leave a reaction chamber 1 mm in length. Reactants (pure allene or allene/Ar in this study) are introduced to the pyrolysis zone through the center-most hole in the inner alumina tube (0.4 mm ID) at rates varying from 0.1 - 1.0 sccm. The reaction zone is resistively heated and temperature within the reactor zone has been calibrated using thermocouples. Thermocouples were not used continuously during experiments due to the catalytic oxidation/pyrolysis observed on the platinum/rhodium wires. Pressure within the microjet reactor was maintained at 600 ± 20 torr. Under the stated operating conditions, wall reactions were not observed to significantly affect product distributions. Significantly lowering the pressure (by a factor of >10), however, leads to greater aromatic abundance at lower temperatures.

A schematic of the VUV photoionization mass spectrometer (VUV-MS) and microjet reactor assembly is illustrated in Figure 1. The TOF-MS is equipped with Wiley-McLaren type acceleration for higher resolution and an ion reflectron to compensate for initial ion energy spread, to provide a longer effective flight length (1 meter) and to prevent the considerable quantities of neutral polymeric hydrocarbons produced from reaching the detector. Mass signals are displayed in real time and recorded directly onto a digital storage oscilloscope which is interfaced with a PC for data analysis. The mass resolution for the experiments described herein was measured as 325 at 78 amu.

VUV photons were generated by the non-linear optical mixing technique of third harmonic generation in Xe. A frequency tripled Nd:YAG laser (Quanta Ray DCR-11 system) operating at 10 Hz was focused into a Xenon cell with a 30 cm path length at 26 torr. The signal from $C_6H_6^+$ produced by single-photon ionization of C_6H_6 from a 300 K fixed flow microjet expansion was used to monitor relative UV to VUV conversion efficiency. Optimum efficiency was found at approximately 30 mJ of energy in a 8 ns pulse at 354.6 nm, corresponding to a peak power of approximately 3.75×10^6 W.

Ionization efficiencies at 118 nm are relatively constant (+/- 35%) and high for many five carbon hydrocarbons and larger, since these compounds have ionization potentials (IPs) of one to two eV below the photon energy (1182 Å =

10.49 eV). Therefore the simultaneously-obtained peak ratios are good approximations of relative concentration. However for smaller hydrocarbons with ionization potentials lying closer to the single photon energy, absorption cross sections and ionization efficiencies vary considerably. Consequently, these species must be calibrated individually. Detection efficiencies of the various molecular hydrocarbons must likewise be considered to obtain quantitative data. These calibration issues have been presented in an earlier publication (5) and are discussed in detail in the PhD thesis of J. Boyle (6).

In our detection scheme only the molecular masses are detected, and the identity of structural isomers can only be inferred from arguments of internal consistency or knowledge of kinetic mechanisms and rate constants.

Experimental Results and Discussion

An overview of the relative concentrations of higher than reactant mass hydrocarbons detected at 2ms mean reaction time is given in Table 1. As temperature was increased from 300K to 1200K at 2ms mean residence time, the first reaction product observed was mass 80 followed at slightly higher temperatures by reaction products smaller than the parent mass such as ethylene. Flow reactor results also indicate methane and hydrogen in significant quantities, although those products were not directly measured in this study due to their high ionization potentials (methane was indirectly measurable through its fragmentation product methyl radical). At 1320K mass 79 was detected above ppm levels and was observed to reach significant steady state concentrations prior to the appearance of mass 78. Benson and Shaw (7a,b) studied the pyrolysis of 1,3 and 1,4-hexadiene at low pressure and temperatures from 520 - 840K. These investigators found that while benzene production from1,4-hexadiene proceeds through molecular elimination of hydrogen, the mechanism for benzene formation from 1,3- hexadiene proceeds via a chain mechanism involving hydrogen atoms, hexadienyl radicals and cyclohexenyl-3 radicals. The rate constant data reported is consistent with our mass 79 and benzene formation rates assuming our experimentally measured mass 80 concentration at 1450K contains a significant component of 1,3-hexadiene. This analysis suggests that a possible pathway for early benzene production during allene pyrolysis involves conversion of 1,2 dimethylenecyclobutane formed through allene dimerization to 1,3-cyclohexadiene as temperature is increased followed by a higher activation energy, slower conversion of cyclohexadiene to benzene through the cyclohexadienyl radical.

As temperature was increased above 1450K a broad range of hydrocarbons with 6 or more carbons were detected including mass 78, with the largest contributions initially coming from masses 91/92, 94, 106, 116-118, 120, 144 and 158. Mass 120 was possibly formed through reaction of a DMCB component of mass 80 with allene as noted in early work on the thermal polymerization of allene. Note that the mass 120 abundance decraeses somewhat with temperature above 1515K. Mass 120 and 160, which are possible allene trimers and tetramers, were not seen in ethylacetylene pyrolysis but are present at significant levels in this study. At 1450K, mass 120 was observed in the next largest abundance to masses 80 and 79. This is another indication of allene dimer formation in this system. The mechanism

illustrated below was reported for allene dimer and trimer formation by Weinstein et al. who identified the structural isomers using NMR.

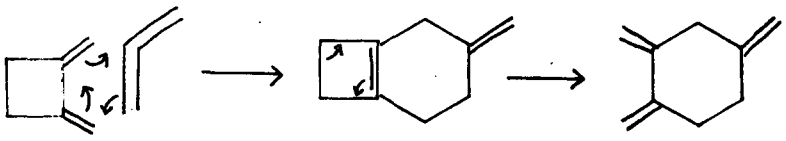

At higher temperatures and allene conversions, these species are converted through reactions with smaller hydrocarbons and hydrocarbon radicals such as C_2H. The early appearance of mass 144 suggests such a route.

Allene dimerization

Thermodynamic parameters for both 1,2 DMCB and 1,3 DMCB were estimated using the THERM program(9) and compared with experimental values where available. For 1,2 DMCB, the DH_{f298} = 47.3 kcal/mol (calculated) and 48 kcal/mol (measured) and for 1,3 DMCB, the DH_{f298} = 51 kcal/mol (calculated) and 53.3 kcal/mol (measured). These values are in good agreement (2-3kcal/mol lower) with the values calculated by Kovacevic and coworkers (10) using the maximum overlap method. These investigators also reported the experimental and calculated strain energy for 1,3 DMCB. From this data, equilibrium constants for the reactions 2Allene $\rightarrow$ 1,2 DMCB and 2Allene $\rightarrow$ 1,3 DMCB were calculated and are presented in Figure 2. The equilibrium constants for both reactions are greater than one at 1200 K. The rate of allene dimerization rate to 1,2-DMCB is pressure dependent and approximately 43.8 Kcal/mol exothermic.

Conclusion

A microjet reactor coupled to vacuum-UV photoionization was used to study the formation of higher hydrocarbons during the pyrolysis of allene. By use of this technique, a progression of intermediate species profiles including hydrocarbon radicals were obtained as a function of temperature at millisecond reaction times. Mass 80 was the first product species observed as temperature was increased which is consistent with early flow reactor studies of allene pyrolysis leading to the formation of predominantly the 1,2 isomer of dimethylenecyclobutane.

Our current work involves an analysis of a proposed mechanistic pathway for conversion allene to 1,2 dimethylenecyclobutane and subsequently to benzene and other higher hydrocarbons. A possible pathway for early benzene production during allene pyrolysis involves allene dimerization to 1,2 dimethylenecyclo-

butane followed by a multistep mechanism converting 1,2-DMCB to 1,3-hexadiene which goes through a higher activation energy, slower conversion mechanism to benzene through the cyclohexadienyl radical. A kinetic analysis using rate data for 1,3-cyclohexadiene to benzene conversion obtained by earlier investigators (7) shows that this route could account for the initial rate of mass 78 production observed experimentally. The higher hydrocarbon product distribution observed in particular the early formation of mass 120 supports the proposed allene dimerization to 1,2-DMCB. Future work will include resolution of mass 80 isomers to aid in the reaction pathway analysis. Data from earlier flow reactor studies can not be used to resolve these issues because of the intrusion of surface effects.

References

1a. Westmoreland, P. R., Dean, A. M., Howard, J. B., and Longwell, J. P., *J. Phys. Chem.* **1989**, 93, 8171-8180; b) F. Communal, S.D. Thomas, and P.R. Westmoreland, "Kinetics of C_3 Routes to Aromatics Formation," Poster P40, 23rd International Symposium on Combustion, Orleans, July 22-27, 1990.

2. Boyle, J., and Pfefferle, L. D., "Methylacetylene and Allene Pyrolysis", presented AIChE Annual Meeting, Chicago Illinois, 12/90.

3. Blomquist, A. T., and Verdol, J. A., *J. Amer. Chem. Soc.*, **1956**, 78, 109-112.

4. Meinert, R.N., and Hurd, C. D., *J. Amer. Chem. Soc.*,**1930**, 52, 4540-4549.

5. Boyle, J., and Pfefferle, L. D., Lobue, J., and Colson, S., *Combust. Sci. and Tech.*, **1990**, 70:187-203.

6. Boyle, J. , PhD thesis, Studies of Pyrolysis and Oxidative Pyrolysis of Allene, Methyl Acetylene, Ethyl Acetylene and Butadiene using VUV Photoionization Mass spectrometry" Yale University, 1991.

7a. Benson, S. W., and Shaw R., *J. Amer. Chem. Soc.*,**1930**, 89:21,5351-4549.

8. Weinstein, B., and Fenselau, A. H., *J. Chem. Soc.* Section C:368-372 (1967).

9. Ritter, E., Bozzelli, J., THERM: Thermo Property Estimation for Radicals and Molecules, Dept. of Chemistry, New Jersey Institute of Technology.

10. Kovacevic, K., Eckert-Maksic, M., and Maksic, Z. B., *Croatica Chemica Acta*, **1974**, 46(4), 249-259.

Acknowledgements

The authors would like to acknowledge discussions about this work with Dr. Kiefer, and partial support from an NSF equipment grant.

Table 1

RELATIVE CONCENTRATIONS OF PRODUCT SPECIES DURING THE PYROLYSIS OF ALLENE 2ms, 600 Torr.

MOLECULAR WEIGHT	TEMPERATURE (K)					
	1280	1320	1450	1515	1545	1580
52	**	**	4.7	4.7	7	12
54	**	**	5.9	29	23	40
56	**	**	8.2	40	56	39
66	**	**	**	3.9	4.3	6
67	**	**	4.0	3.9	3.5	3.5
68	**	**	**	4.3	4.3	5
78		*	3.1	23	31	47.5
79		1.5	17	30	35	43.5
80	2.4	5	25	43	50.5	52
91			2.3	2	3.5	5.5
92			3.1	22	35	30
93			---	*	6	9.8
94			3.9	14	15	19.6
104			---	2.7	6.3	8.6
105				5.5	5.5	8.5
106			2.4	12.5	12	22
116				5.9	9.5	11.3
117			---	4.7	7.5	14
118				9.8	14	23
120			7.8	20.5	18	19
128					6.2	10
130					10.5	14
142				9	14.5	17
144			2.7	7	13	14.5
154					2	4
156				7	15	21
158			3.5	6.3	10.5	12
160				10	5	5
166					5	6
168						8.5
170					5	10
178					1	3
180					4.3	10

* Species present in 0-1 unit
** Species present in 1-2 units
Note: Only those hydrocarbon radical species with comparable concentration to the stable analog were included in this table.

Figure 1: Schematic of the VUV Photoionization Mass Spectrometer and Microjet Reactor Experiment

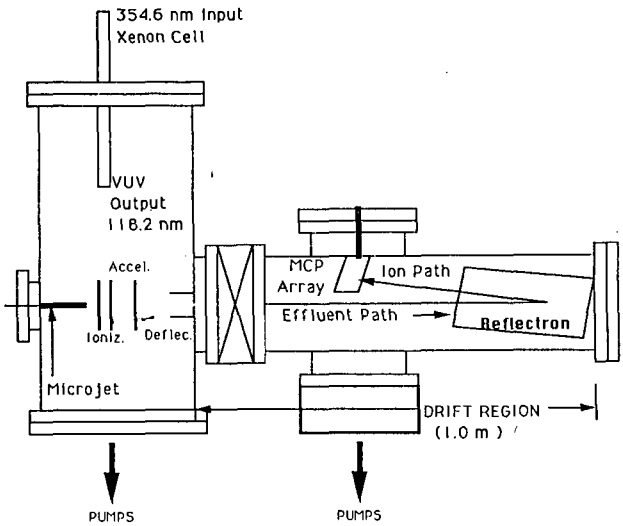

Figure 2: Equilibrium Constants for the Dimerization of Allene to the 1,2- and 1,3- Isomers of Dimethylenecyclobutane